Doctoral Dissertation (Shinshu University)

Smart Nanofibrous Nonwovens Fabricated by Electrospinning

March 2013

Qiang Gao

CHAPTER 1 General introduction

1.1 Definition of nanofiber

With the rapid development of nanotechnology, there have been a significantly increasing number of studies on nanofibers and their applications. The International Standards Organization (ISO) considers nanomaterials to be materials that are typically but not exclusively below 100 nm in at least one dimension. However, in informal nonwovens, textile, and other engineered fibers industries, it has been well accepted that nanofibers are fibers with the diameter smaller than 1000 nm [1, 2]. In 1992, carbon nanofibers were discovered to grow spontaneously by deposition from carbon vapor [3]. After that, many other techniques have been developed to fabricate nanofibers such as electrospinning [4, 5], self-assembly [6, 7], phase separation [8, 9], etc. Due to the nanoscale diameter, nanofibers possess high-surface-to-volume ratios which help to enhance interactions between the nanofibers and targeted substrates in different fields compared to other micro- to macro-size materials. Thus, employing nanofibers could be a promising approach for the advanced developments in science and technology. In this chapter, we aim to summarize the techniques for producing nanofibers and recent achievements in their applications.

1.2 Fabrication methods of nanofibers

1.2.1 Electrospinning

Electrospinning is a technique using electrostatic forces to fabricate nanofibers. As shown in Figure1-1, when a high voltage is applied to the droplet of a polymer solution, the molecules of the solution becomes charged and an electrostatic repulsion occurs, which counteracts the surface tension of the droplet. When the high voltage increases to a critical point, a jet of the solution is erupted from the liquid surface. As the solvent evaporates, further stretching of the charged jet under the electrostatic forces will push it into a bending instability stage. The elongation and thinning of the charged jet due to this instability lead to the formation of continuous fibers with diameters in nanoscale. Based on this principle, different electrospinning setups as well as different types of collectors have been designed to create various nanofibrous architectures [4, 5].
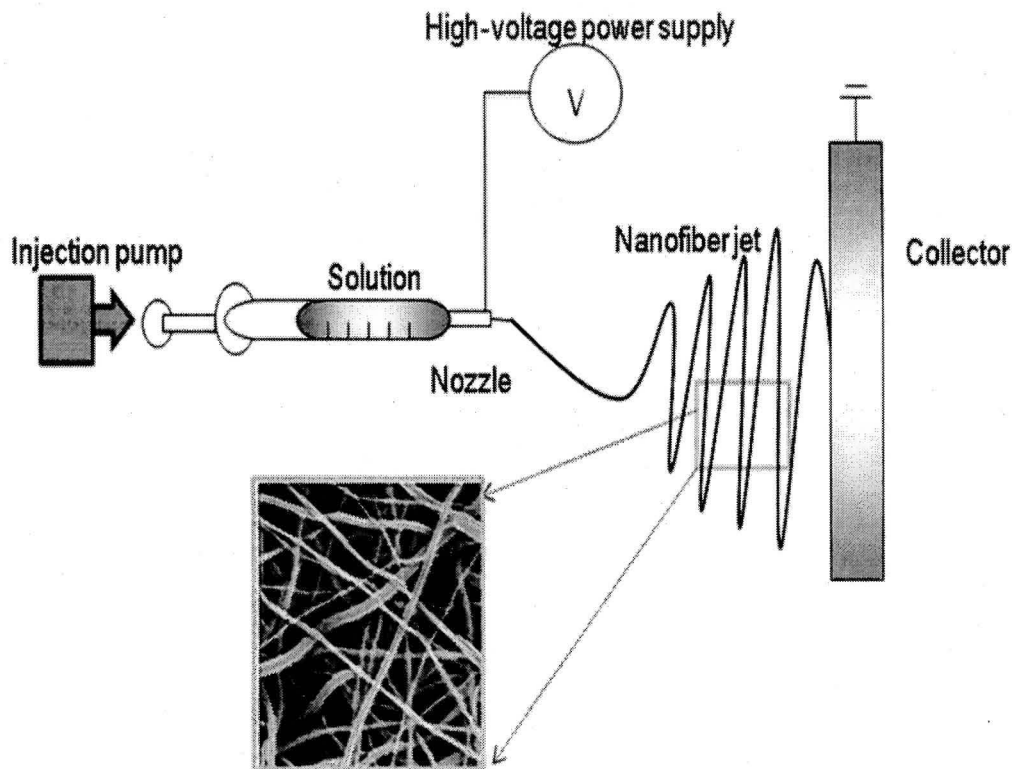
Figure1-1 The process of electrospinning

The shapes and dimensions of the fibers formed depend on a large set of parameters, for example, the properties of the polymer itself (such as molecular weight, molecular-weight distribution, and solubility), as well the properties of the polymer solution (such as viscosity, surface tension, and electrical conductivity) [4]. The vapor pressure of the solvent and the relative humidity of the surroundings can also have a significant impact. Furthermore, the properties of the substrate, the feed rate of the solution, and the field strength and geometry of the electrodes (and therefore, the form of the electric field) play a major role in fiber formation. Lower diameter fibers with uniform morphologies were prepared by electrospinning of poly(vinylidene fluoride) (PVDF) with tetrabutylammonium chloride (TBAC), whereby TBAC increased the electrical conductivity of the solution [10]. Electrically induced double layer in combination with the polyelectrolytic nature of solution was also anticipated as a method for formation of high-aspect-ratio polyamide-6 nanofibers with diameters as small as 9-28 nm [11].

Commonly, randomly oriented fibers are deposited on a flat collector plate forming a nonwoven mat of fibers. Another approach commonly applied is using a spinneret containing two needles to produce composite nanofibers [12]. Moreover,

many different types of molecules can be incorporated into the fibers and a wide range of polymers are electrospun in varying fiber diameters ranging from <100 nm to micrometer levels via electrospinning. Controlled fiber deposition techniques are also applied for the preparation of aligned nanofibers, on a rotation drum or a rotating disk. Using a collector designed of two conductive strips separated by a void gap of desired width, uniaxially aligned nanofibers were produced too. The alignment of the fibers could induce cell elongation and reorganize the cytoskeletal structures that regulate the cell adhesion and morphology. However, electrospinning has limitations of low productivity, as solutions are usually fed at a low rate so as to produce fibers of low diameter.

Various structural variations of the nanofibers include careful design of core-shell nanofibers, porous scaffolds or even multilayered fiber structures. Electrospun nanofibers of these architectures can act as drug delivery reservoirs for controlled and timely release of drugs, proteins, antioxidants, and other molecules to the site of tissue repair. The use of molten polymers to produce electrospun mats introduced as "melt electrospinning" is an environmentally benign process since it implies a solvent free approach [13]. Cellular infiltration within the electrospun scaffold remains a great challenge and methods such as cell electrospraying are also concurrently performed during the fabrication of a vascular conduit [14]. Benefits of electrospinning technique are plenty, but challenges of obtaining a three-dimensional (3D) scaffold by electrospinning still remains a field of exploration.

Nanofibrous and microfibrous 3D scaffolds of desired shape and size are more preferred as implantable materials compared to the electrospun 2D scaffolds. Compared to electrospinning, the major advantage of self-assembly is that it can produce fine nanofibers smaller than 10 nm and these nanofibers could be applied as injectable scaffolds for tissue regeneration. Pore sizes (interspace among nanofibrous mats) of 5-200 nm are insufficient for cell migration and proliferation [15]. In this respective, both electrospinning and self-assembly have one common drawback, of incapability to control the pore size and pore structure of the scaffolds. The challenge to integrate nanofibers into useful devices requires well-controlled orientation, size, and other target characteristics of the nanofibers. Reproducibility in locating them in specific positions and orientations still remain to be faced.

1.2.2 Self assembly

Self-assembly is a type of process in which a disordered system of pre-existing components forms an organized structure or pattern as a consequence of specific, local interactions among the components themselves, without external direction. When the constitutive components are molecules, the process is termed molecular self-assembly. For nanofiber fabrication, self assembly is a bottom-up process in which small molecules spontaneously assemble into well-ordered nanofibers. The formation of this structure is induced by many interactions, including π–π stacking, hydrogen bonds, non-specific vander Waals interactions, electrostatic interactions, and repulsive steric forces [6]. Normally, the basic molecules to fabricate nanofibers using this technique are peptide amphiphiles (PA). They consist of a dialkyl chain moiety (hydrophobic component/tail group) attached to an N-a-amino group of a peptide chain (hydrophilic component/head group) [7]. The peptides can be self-assembled by many reagents such as acid, divalent ion, and covalent capture, etc [6].

Bioactive sequences were introduced within PA with formation of the triple helix structure by Malkar et al [16] and it demonstrated much similarity to the native self-assembled triple helix of the extracellular matrix (ECM). The self-assembly of PAs into nanofibers was developed by engineering of the peptide head group of the PA by controlling the pH of the solution [17]. With advances in this field, even the osteogenic differentiation of mesenchymal stem cells (MSCs) was possible in self-assembled PA nanofibers containing RGD peptide sequences [18]. Moreover, PAs can be self-assembled reversibly into nanofibers and hence it could be applied, for versatile material fabrications. It produced nanofibers in high yield with low polydispersity, enabling further exploration of this method for developing "smart" biomaterial scaffolds for effective tissue regeneration.

1.2.3 Phase separation

Thermally induced phase separation was commonly employed during the early days to produce porous polymeric scaffolds. The method was explored further to produce nanofibrous 3D structures from a variety of biodegradable polymers by Ma and Zhang *et al.* [8, 9]. Scaffolds with porous structure and interconnected spaces are greatly suitable for implantation, mainly because the continuous fibrous network

provide interconnecting mechanical support for cell attachment, proliferation, and migration [19]. The selection of proper solvent is considered as one of the most critical step of nanofibrous structure formation during this process. The formation of the nanofibrous structure is postulated to be caused by spinodal liquid-liquid phase separation of the polymer solutions and consequential crystallization of the polymer rich phase. The method does not require specialized instruments and it also allows for batch to batch consistency, while the architecture and scaffold properties can be controlled easily by varying the polymer concentration, gelation temperature/time, solvent, and freezing temperature [8, 9]. Such 3D macroporous structures are advantageous to the cells to absorb nutrients, receive signals, and to discard wastes. The presence of both nano- and macro-structures at the nanofiber level provides additional benefits to cell distribution and response [9].

Table 1-1. Advantages and disadvantages of fabrication methods of nanofibers.

Fabrication approach	Advantages	Disadvantages
Electrospinning	1. nanofibers are long and continuous 2. flexibility in material selection 3. various architectures or patterns can be created, bulk structure can be formed	1. small pore size[15] 2. difficult to get fibers with diameter less than 50 nm
Self-assembly	setup was not needed	1. limited material selection 2. only short nanofibers (usually less than mm scale) can be fabricated
Phase separation	simple bulk structure can easily be formed	limited material selection

1. 3 Applications of nanofibers via electrospinning

1.3.1 For composites applications

One of the most important applications of conventional fibers, especially engineering fibers such as carbon, glass, and Kevlar fibers, is to be used as reinforcement fillers in composite developments [20]. With these reinforcements, the composite materials can provide superior structural properties such as high modulus and strength to weight ratios, which generally cannot be achieved by other engineered monolithic materials alone. Thus, nanofibers will also eventually find important applications in making nanocomposites. This is because nanofibers can have even better mechanical properties than micro fibers of the same materials, and hence the superior structural properties of nanocomposites can be anticipated. Moreover, nanofiber reinforced composites may possess some additional merits which cannot be shared by conventional (microfiber) composites. For instance, if there is a difference in refractive indices between fiber and matrix, the resulting composite becomes opaque or nontransparent due to light scattering. This limitation, however, can be circumvented when the fiber diameters become significantly smaller than the wavelength of visible light [21]. Perhaps the majority work in the current literature on nanofiber composites is concerned with carbon nanofiber or nanotube reinforcements. These nanofibers or nanotubes are generally not obtained through electrospinning.

Several comprehensive reviews have summarized the researches done until very recently on these composites [22-25]. On the other hand, so far polymer nanofibers made from electrospinning have been much less used as composite reinforcements. Only limited researchers have tried to make nanocomposites reinforced with electrospun polymer nanofibers. Information on the fabrication and structure-property relationship characterization of such nanocomposites is believed to be useful, but is unfortunately not much available in the literature. Reneker [26] investigated the reinforcing effect of electrospun nanofibers of polybenzimidazole (PBI) in an epoxy matrix and in a rubber matrix. The PBI polymer was electrospun into non-woven fabric sheets, which were treated with aqueous sulfuric acid and other procedures for composite fabrication [27]. The rubber matrix was mixed with the chopped fiber fabrics which were made by cutting the nonwoven nanofiber sheets

into 0.5 cm squares, and was compression molded into composite samples. Fiber contents of 3-15% by weight were determined by extracting the fibers from the uncured mixture with toluene. Tensile, 3-point bending, double torsion, and tear tests were performed for the epoxy and rubber nanocomposites, respectively. As the tested samples were in normal dimensions, relevant testing standards were followed. It was found that with increasing content of fibers, the bending Young's modulus and the fracture toughness of the epoxy nanocomposite were increased marginally, whereas the fracture energy increased significantly. For the rubber nanocomposite, however, the Young's modulus was ten times and the tear strength was twice as large as that of the unfilled rubber material. Bergshoef and Vancso fabricated a nanocomposite using electrospun Nylon-4, 6 nanofiber nonwoven membranes and an epoxy matrix [28]. After electrospinning, the membranes were washed with ethanol and dried at room temperature and atmospheric pressure, and then were impregnated with the epoxy resin by dipping them into the diluted resin. The composite film samples were obtained after the resin impregnated membranes were cured at room temperature. Tensile tests were conducted for the composite as well as the monolithic matrix films. It was reported that both the stiffness and strength of the composite were significantly higher than those of the reference matrix film although the fiber content was low. A US patent was issued to Dzenis and Reneker [29] who proposed using polymer nanofibers in between laminas of a laminate to improve delamination resistance. They arranged PBI nanofibers at the interfaces between plies of the laminate without a substantial reduction for the in-plain properties and an increase in weight and/or ply thickness.

It was reported that by incorporating electrospun PBI nanofibers of 300-500 nm diameters in-between a unidirectional composites made of graphite/epoxy prepregs of T2G190/F263, Mode I critical energy release rate G_{Ic} increased by 15%, while an increase of 130% in the Mode II critical energy release rate G_{IIc} was observed. Up to date, the polymer composites reinforced with electrospun nanofibers have been developed mainly for providing some outstanding physical (e.g. optical and electrical) and chemical properties while keeping their appropriate mechanical performance. For instance, in the report by [21], the epoxy composite with electrospun nylon 4, 6 nanofibers of 30-200 nm diameters exhibited a characteristic transparency due to the

fiber sizes smaller than the wavelength of visible light. It is also noted that single wall carbon nanotube (SWNT) reinforced polyimide composite in the form of nanofibrous film was made by electrospinning to explore a potential application for spacecrafts [30]. Carbon nanofibers for composite applications can also be manufactured from precursor polymer nanofibers [31-35]. Such kind of continuous carbon nanofiber composite also has potential applications as filters for separation of small particles from gas or liquid, supports for high temperature catalysts, heat management materials in aircraft and semiconductor devices, as well as promising candidates as small electronic devices, rechargeable batteries, and supercapacitors [36-50].

Due to limited number of papers published in the open literature, many important issues relevant to nanocomposites reinforced with electrospun polymer nanofibers have essentially not been taken into account yet. For instance, it is well known that the interface bonding between a polymer fiber and a different polymer matrix is generally poor. How to modify this bonding for polymer nanofiber polymer matrix composites seems to have not been touched at all, although there are a vast number of publications on this topic for traditional fibrous composites in the literature. Furthermore, little work has been done on the modeling and simulation of the mechanical properties of nanofiber composites. Although many micromechanics models have been developed for predicting the stiffness and strength of fibrous composites [51], whether they are still applicable to nanofiber composites needs to be verified [52]. Compared with its counterpart for conventional fibrous composites, one of the main barriers to the implementation of such work for nanofiber composites is that one does not know the mechanical behavior of single polymer nanofibers.

Several reasons can be attributed to the less development of electrospun polymer nanofiber reinforced composites. First of all, not sufficient quantity of uniaxial and continuous nanofibers has been obtained and could be used as reinforcements. It is well known from composite theory and practice that the superior structural properties can be achieved only when fibers are arranged in pre-determined directions such as in unidirectional laminae, multidirectional laminates, woven or braided fabric reinforced composites. To make these composites, continuous fiber bundles are necessary. The nonwoven or randomly arranged nanofiber mats, as collected to date

from electrospinning, generally cannot result in a significant improvement in the mechanical properties of the composites with their reinforcement. Another reason may be that polymers yielding these fibers are generally considered as less suitable for structural enhancement. Although carbon nanofibers are principally achievable from post-processing of electrospun precursor polymer nanofibers such as polyacrylonitrile (PAN) nanofibers [53-54], these fibers seem to have not been obtained in large quantity of continuous single yarns yet. Thus, extensive workboth from the standpoint of nanofiber composite science (fabrication, characterization, modeling and simulation) and from industrial base (applications) viewpoint is necessary in the future.

1.3.2 For biomedical applications

Almost all of the human tissues and organs are deposited in nanofibrous forms or structures. Examples include: bone, collagen, cartilage, and skin. All of them are characterized by well organized hierarchical fibrous structures realigning in nanometer scale. As such, current research in electrospun polymer nanofibers has focused one of their major applications on bioengineering. We can easily find their promising potential in various biomedical areas.

a. Medical prostheses

Polymer nanofibers fabricated via electrospinning have been proposed for a number of soft tissue applications such as blood vessel, vascular, breast, etc. [55-61].In addition, electrospun biocompatible polymer nanofibers can also be deposited as a thin porous film onto a hard tissue prosthetic device designed to be implanted into the human body [62-64]. This coating film with gradient fibrous structure works as an interphase between the prosthetic device and the host tissues, and is expected to efficiently reduce the stiffness mismatch at the tissue/device interphase and hence prevent the device failure after the implantation.

b. Tissue template

For the treatment of tissues or organs in malfunction in a human body, one of the challenges to the field of tissue engineering/biomaterials is the design of ideal scaffolds/synthetic matrices that can mimic the structure and biological functions of the natural extracellurlar matrix (ECM). Human cells can attach and organize well around fibers with diameters smaller than those of the cells [65]. In this regard,

nanoscale fibrous scaffolds can provide an optimal template for cells to seed, migrate, and grow. A successful regeneration of biological tissues and organs calls for the development of fibrous structures with fiber architectures beneficial for cell deposition and cell proliferation. Of particular interest in tissue engineering is the creation of reproducible and biocompatible three-dimensional scaffolds for cell ingrowth resulting in bio-matrix composites for various tissue repair and replacement procedures.

Recently, people have started to pay attention to making such scaffolds with synthetic biopolymers and/or biodegradable polymer nanofibers [66-81]. It is believed that converting biopolymers into fibers and networks that mimic native structures will ultimately enhance the utility of these materials as large diameter fibers do not mimic the morphological characteristics of the native fibrils.

c. Wound dressing

Polymer nanofibers can also be used for the treatment of wounds or burns of a human skin, as well as designed for haemostatic devices with some unique characteristics. With the aid of electric field, fine fibers of biodegradable polymers can be directly sprayed/spun onto the injured location of skin to form a fibrous mat dressing Fig. 1-2, which can let wounds heal by encouragingthe formation of normal skin growth and eliminate the formation of scar tissue which would occur in a traditional treatment [82-84]. Non-woven nanofibrous membrane mats for wound dressing usually have pore sizes ranging from 500 nm to 1 mm, small enough to protect the wound from bacterial penetration via aerosol particle capturing mechanisms. High surface area of 5-100 m^2/g is extremely efficient for fluid absorption and dermal delivery.

Figure 1-2. Nanofibers for wound dressing (www.electrosols.com)

d. Drug delivery and pharmaceutical composition

Delivery of drug/pharmaceuticals to patients in themost physiologically acceptable manner has always been an important concern in medicine. In general, the smaller the dimensions of the drug and the coating material required to encapsulate the drug, the better the drug to be absorbed by human being. Drug delivery with polymer nanofibers is based on the principle that dissolution rate of a particulate drug increases with increasing surface area of both the drug and the corresponding carrier if needed. Kenawy *et al.* investigated delivery of tetracycline hydrochloride based on the fibrous delivery matrices of poly (ethylene-co-vinylacetate), poly(lactic acid), and their blend [85]. In another work by [86], bioabsorbable nanofiber membranes of poly(lactic acid) targeted for the prevention of surgeryinduced adhesions, ware also used for loading an antibiotic drug Mefoxin. Preliminary efficiency of this nanofiber

membrane compared with bulkfilm was demonstrated. Ignatious and Baldoni [87] described electrospun polymer nanofibers for pharmaceutical compositions, which can be designed to provide rapid, immediate, delayed, or modified dissolution, such as sustained and/or pulsatile release characteristics. As the drug and carrier materials can be mixed together for electrospinning of nanofibers, the likely modes of the drug in the resulting nanostructed products are: (1) drug as particles attached to the surface of the carrier which is in the form of nanofibers, (2) both drug and carrier are nanofiber-form, hence the end product will be the two kinds of nanofibers interlaced together, (3) the blend of drug and carrier materials integrated into one kind of fibers containing both components, and (4) thecarrier material is electrospun into a tubular form in which the drug particles are encapsulated. The modes (3) and (4) may be preferred. However, as the drug delivery in the form of nanofibers is still in the early stage exploration, a real delivery mode after production and efficiency have yet to be determined in the future.

e. Cosmetics

The current skin care masks applied as topical creams, lotions or ointments may include dusts or liquid sprays which may be more likely than fibrous materials to migrate into sensitive areas of the body such as the nose and eyes where the skin mask is being applied to the face. Electrospun polymer nanofibers have been attempted as a cosmetic skin care mask for the treatment of skin healing, skin cleansing, or other therapeutical or medical properties with or without variousadditives [88]. This nanofibrous skin mask with very small interstices and high surface area can facilitate far greater utilization and speed up the rate of transfer of the additives to the skin for the fullest potential of the additive. The cosmetic skin mask from the electrospun nanofibers can be applied gently and painlessly as well as directly to the three-dimensional topography of the skin to provide healing or care treatment to the skin.

f. Protective clothing application

The protective clothing in military is mostly expected to help maximize the survivability, sustainability, and combat effectiveness of the individual soldier systemagainst extreme weather conditions, ballistics, and NBC (nuclear, biological, and chemical) warfare [89-96]. In peace ages, breathing apparatus and protective clothing with the particular function of against chemical warfare agents such as sarin,

soman, tabun and mustard gas from inhalation and absorption through the skin become special concern for combatants in conflicts and civilian populations in terrorist attacks. Current protective clothing containing charcoal absorbents has its limitations in terms of water permeability, extra weight-imposed to the article of clothing. As such, a lightweight and breathable fabric, which is permeable to both air and water vapor, insoluble in allsolvents and highly reactive with nerve gases and other deadly chemical agents, is desirable. Because of their great surface area, nanofiber fabrics are capable of the neutralization of chemical agents and without impedance of the air and water vapor permeability to the clothing [97-100]. Electrospinning results in nanofibers laid down in a layer that has high porosity but very small pore size, providing good resistance to the penetration of chemical harm agents in aerosol form [101-110]. Preliminary investigations have indicated that compared to conventional textiles the electrospun nanofibers presentboth minimal impedance to moisture vapor diffusion and extremely efficiency in trapping aerosol particles [102,106,111-113], as well as show strong promises as ideal protective clothing.

1.3.3 For electrical and optical application

Conductive nanofibers are expected to be used in the fabrication of tiny electronic devices or machines such as Schottky junctions, sensors and actuators. Due to the well-known fact that the rate of electrochemical reactionsis proportional to the surface area of the electrode, conductive nanofibrous membranes are also quite suitablefor using as porous electrode in developing high performance battery [114-127]. Conductive (in terms of electrical, ionic and photoelectric) membranes also have potential for applications including electrostatic dissipation, corrosion protection, electromagnetic interference shielding, photovoltaic device, etc. [128-139]. Waters *et al.* [140] reported to use electrospun nanofibers in the development of a liquid crystal device of optical shutter which is switchable under an electric field between a state in which it is substantially transparent to incident light and a state in which it is substantially opaque. The main part of this liquid crystal device consisted of a layer of nanofibers permeated with a liquid crystal material, having a thickness of only few tens microns. The layer was located between two electrodes, by means of which an electric field could be applied across the layer to vary the transmissivity of the liquid crystal/nanofiber composite. It is the fiber size

used that determines the sensitivities of the refractive index differences between the liquid crystal material and the fibers, and consequently governs the transmissivity of the device. Obviously nanoscale polymer fibers are necessary in this kind of devices.

1.3.4 For other application

Nanofibers from polymers with piezoelectric effect such as polyvinylidene fluoride will make the resultant nanofibrous devices piezoelectric. Electrospun polymer nanofibers could also be used in developing functional sensors with the high surface area of nanofibers facilitating the sensitivity. Poly (lactic acid co glycolic acid) nanofiber films were employed as a new sensing interface for developing chemical and biochemical sensor applications [141,142]. Highly sensitive optical sensors based on fluorescent electrospun polymer nanofiber films were also recently reported [143-155]. Preliminary results indicate the sensitivities of nanofiber films to detect ferric and mercury ions and a nitro compound (2,4-dinitrotulene, DNT) are two to three orders of magnitude higher than that obtained from thin film sensors. Nanoscale tubes made from various materials including carbon, ceramics, metals, and polymers are important in many industry fields. Ultrafine fibers prepared from electrospinning can be used as templates to develop the various nanotubes [156,157]. In general, the tube material is coated on the nanofiber template, and the nanotube is formed once the template is removed through thermal degradation or solvent extraction. For this purpose, the template nanofiber must be stable during the coating and be degradable or extractable without destructing the coating layer. By using PLA nanofibers, Bognitzki *et al.* obtained polymer [PPX, or poly(p-xylylene)], composite of polymer (PPX) and metal, and metal (aluminum) nanotubes respectively through chemical vapor deposition (CVD) coating and physical vapor deposition (PVD) coating and then thermal degradation. The wall thickness of the tubes was in the range of 0.1-1mm [156]. Hou *et al.* employed the similar procedure. However, both PA [poly (tetramethylene adipamide)] and PLA nanofiber of smaller diameters were used as templates and thinner nanotubes were achieved [157].

1.4 Objective of this study

The extremely small diameters (~ nm) and high surface to volume and aspect ratios found in electrospun fibers have been well recognized. Previous studies mainly focus on the morphology or structure of electrospun nanofibers. This thesis disclosed

new specialties of nanofibers by using the nanosize effect of electrospun fibers. It includes two issues as follows.

Firstly, the nanofibrous morphology which contributes to the high surface area not stable in many aqueous conditions which limit their applications. This thesis contains the approach to fabricate tough nanofibers which can maintain their nanofibrous morphology with hydrophilic surface. Secondly, compare to the nanoparticles, the electrospun nanofibers could be in some aligned assembles or patterns which might reveal new functionalities of pristine materials. Meanwhile, challenges to explore new applications of aligned assembles were covered. According to the main objectives, polyvinyl alcohol (popular nonconductive synthetic polymer) and poly(3-hexylthiophene) (widely-used semiconductive polymer) were selected in this thesis.

PVA is a colourless, water-soluble synthetic resin employed principally in the treating of textiles and paper. Since the production of PVA is multi-step process, the monomer source, polymerization route and saponification process may give rise to PVA with the differences in molar mass, tacticity, and metal ion impurity and so on. The effects of di or trivalent metal ions on electrospinning process haven't been paid any attention yet, however, the di- and trivalent metal ions can substantially change the viscosity, electricconductivity and surface tension of aqueous PVA solutions because PVA can physically interact with these metal ions.

In chapter 2, improving the electrospinning process of polyvinyl alcohol (PVA) which contained impurity of high metal ions aqueous solutions was done by dialysis and complexation pretreatment.

In chapter 3, the inter-relationship between metal ions and high saponification degree on electrospinning were further studied in detail.

While PVA electrospun nanofibers have been prepared by the electrospinning method and investigated their functions [158-165], PVA nanofibers can not maintain their fibrous morphology in water owing to high hydrophilicity of PVA. Chemical cross-linking of PVA fibers can also improve its stability. Glutaraldehyde, maleic anhydride, glyoxal, and blocked isocyanate prepolymer have been investigated as chemical cross-linking agents for PVA nanofibers. However, harmful acids should be used as catalyst and these fiber morphologies were changed after immersed in water at room temperature.

In chapter 4, the preparation of PVA nanofibers cross-linked with *N,N'*-trimethylene-bis[2-(vinylsulfony) acetamide] was reported. *N,N'*-trimethylene-bis[2-(vinylsulfony) acetamide] has been used for the preparation of water-insoluble materials by the formation of cross-linking points among water-soluble polymers including gelatins and starches. The vinylsulfonyl groups react with hydroxy groups in PVA without the use of catalytic acid. The aqueous mixture of PVA and *N,N'*-trimethylene-bis[2-(vinylsulfony) acetamide] at room temperature do not cause gelation by the formation of cross-linking points and keep stable solution having the same viscosity during one month. This indicates that the cross-linking reaction does not occur in aqueous solution. On the other hand, the dried PVA films prepared from aqueous solution of PVA and *N,N'*-trimethylene-bis[2-(vinylsulfony) acetamide] exhibits insoluble in water after the thermal treatment at 150 °C. Compound *N,N'*-trimethylene-bis[2-(vinylsulfony) acetamide] is suitable as a cross-linking agent to obtain *in situ* cross-linked PVA nanofibers though the electrospinning process. Hot water resistant PVA nanofibers were fabricated and using them as the template for deposition of functional nanoparticles.

In chapter 5, In order to achieve well-aligned nanofiber assembles and explore the new features of nanofibrous patterns, P3HT was chose to challenge this issue. Regioregular poly (3-alkylthiophene)s (P3HTs) are the most prominent organic semiconductors applied in organic electronics involving organic field-effect transistors and solar cells [166]. Because of the absence of chain entanglement of rigid rod-like P3HT in a solution, the continuous electrospinning of uniform P3HT nanofibers requires either mixing with high-molecular-weight insulating polymers or the use of highly concentrated solutions [167-170]. Pristine P3HT electrospun fiber by using a high-molecular-weight regioregular P3HT was reported. The molecular weight of this P3HT is about 10 times higher than that of the P3HT used in previous studies. Our expectation was that the longer length of the rigid P3HT backbone would increase the solution viscosity of a low-concentrated solution. This change of solution property may improve the electrospinning stability in the fabrication of pure P3HT nanofibers.

References

[1] Klaessig F, Marrapese M, Abe S, "Current Perspectives in Nanotechnology Terminology and Nomenclature," in Nanotechnology Standards, (Eds., V. Murashov, J. Howard), Springer Verlag, New York, 2011, 260.

[2] Greiner A, Wendorff JH, *Angew. Chem. Int. Ed.*, 2007, *46*, 5670-5703.

[3] Endo M, Kroto HW, *J. Phys. Chem.*, 1992, *96*, 6941-6944.

[4] Fong H, Chun I, Reneker DH, *Polymer*, 1999, *40*, 4585-4592.

[5] Teo WE, Ramakrishna S, *Nanotechnology*, 2006, *17*, R89.

[6] Hartgerink JD, Beniash E, Stupp SI, *Proc. Natl. Acad. Sci. U.S.A.*, 2002, *99*, 5133-5138.

[7] Berndt P, Fields G, Tirrell M, *J. Am. Chem. Soc.*, 1995, *117*, 9515-9522.

[8] Ma PX, Zhang R, *J. Biomed. Mater. Res.*, 1999, *46*, 60-72.

[9] Ma P, Choi J, *Tissue Eng.*, 2001, *7*, 23-33.

[10] Yee WA, Kotaki M, Liu Y, Lu XH, *Polymer*, 2007, *48*, 512-521.

[11] Nirmala R, Nam KT, Park SJ, Shin YS, Navamathavan R, Kim HY, *Appl. Surf. Sci.*, 2010, *256*, 6318-6323.

[12] Gupta P, Wilkes GL, *Polymer*, 2003, *44*, 6353-6359.

[13] Zhou H, Greenc TB, Jooa Y L, *Polymer*, 2006, *47*, 7497-7505.

[14] Stankus JJ, Soletti L, Fujimoto K, Hong Y, Vorp DA, Wagner WR, *Biomaterials*, 2007, *28*, 2738-2749.

[15] Zhang S, Holmes TC, DiPersio CM, Hynes RO, Su X, Rich A, *Biomaterials*, 1995, *16*, 1385-1384.

[16] Malkar NB, Lauer-Fields JL, Juska D, Fields GB, *Biomacromolecules*, 2003, *4*, 518-524.

[17] Hartgerink JD, Beniash S, Stupp I, *Science*, 2001, *294*, 1684-1690.

[18] Hosseinkhani H, Hosseinkhani M, Tian F, Kobayashi H, Tabata Y, *Biomaterials*, 2006, *27*, 4079-4085.

[19] Shin M, Abukawa H, Troulis MJ, Vacanti JP, *J. Biomed. Mater. Res. A*, 2008, *84*, 702-710.

[20] Chand S, *J. Mater. Sci.*, 2000, *35*, 1303-1313.

[21] Bergshoef MM, Vancso GJ, *Adv. Mater.*, 1999, *11*, 1362-1365.

[22] Baughman RH, Zakhidov AA, de Heer WA, *Science*, 2002, *297*, 787-792.

[23] Maruyama B, Alam K. *SAMPE. J.*, 2002, *38*, 59-70.

[24] Thostenson ET, Ren ZF, Chou TW, *Comp. Sci. & Tech.*, 2001, *61*,1899-1912.

[25] Lau KT, Hui D. *Composites Part B*, **2002**, *33*, 263-277.

[26] Kim JS, Reneker DH, *Polymer Composites*, **1999**, *20*,124-131.

[27] Kim JS. *PhD dissertation*, The Graduate Faculty of the University of Akron, **1997**.

[28] Bergshoef MM, Vancso GJ, *Adv. Mater.*, **1999**, *11*, 1362-1365.

[29] Dzenis YA, Reneker DH. *US Patent*, No. 626533, **2001**.

[30] Park C, Ounaies Z, Watson KA, Pawlowski K, Lowther SE, Connell JW, Making Functional Materials with Nanotubes Symposium (*Materials Research Society Symposium Proceedings*), **2002**, *706*, 91-96.

[31] Chun I, Reneker DH, Fong H, Fang X, Deitzel J, Tan NB, et al. *Journal of Advanced Materials*, **1999**, *31*, 36-41.

[32] Dzenis YA, Wen YK. *Materials Research Society Symposium-Proceedings*, **2002**, *702*, 173-178.

[33] Wang Y, Serrano S, Santiago-Aviles JJ, *Synth. Met.*, **2003**, *38*, 423-427.

[34] Wang Y, Santiago-Aviles JJ, *J. Appl. Phys.*, **2003**, *94*, 1721-1727.

[35] Ko F, Gogotsi Y, Ali A, Naguib N, Ye H, Yang G, Li C, Willis P, *Adv. Mater.*, **2003**, *15*, 1161-1165.

[36] Han H, Song T, Bae JY, Nazar LF, Kim H, Paik U, *Energy Environ. Sci.*, **2011**, *4*, 4532-4536.

[37] Ji L, Jung KH, Medford A, Zhang XW, *J. Mater. Chem.*, **2009**, *19*, 4992-4997.

[38] Ji L, Zhang X, *Electrochem. Commun*, **2009**, *11*, 795-798.

[39] Wang L, Yu Y, Chen P, Zhang D, Chen C, *J. Power Sources*, **2008**, *183*, 717-723.

[40] Wang L, Yu Y, Chen PC, Chen CH, *Scr. Mater.*, **2008**, *58*, 405-411.

[41] Yu Y, Gu L, Zhu C, Van Aken P, Maier J, *J. Am. Chem. Soc.*, **2009**, 131, 15984-15985.

[42] Yu Y, Gu L, Wang C, Dhanabalan A, Van Aken P, Maier J, *Angew. Chem. Int. Ed.*, **2009**, *48*, 6485-6489.

[43] Ding Y, Zhang P, Long Z, Jiang Y, Xu F, *J. Alloys Compd.*, **2009**, *487*, 507-510.

[44] Fan X, Zou L, Zheng YP, Kang FY, Shen WC, *Electrochem. Solid-State Lett.*, **2009**, *12*, A199-201.

[45] Ji L, Lin Z, Zhou R, Shi Q, Toprakci O, Medford A, Millns CR, Zhang X,

Electrochim. Acta, **2010**, *55*, 1605-1611.

[46] Ji L, Lin Z, Medford A, Zhang X, *Chem. Eur. J.*, **2009**, *15*, 10718-10722.

[47] Ji L, Zhang X, *Nanotechnology*, **2009**, *20*,155705.

[48] Lu HW, Yu L, Zeng W, Li YS, Fu ZW, *Electrochem. Solid State*, **2008**, *11*, A140-144.

[49] Gu Y, Chen D, Jiao X, *J. Phys. Chem. B*, **2005**, *109*, 17901-17906.

[50] Gu Y, Chen D, Jiao X, Liu F, *J. Mater. Chem.*, **2007**, *17*, 1769-1776.

[51] Huang ZM, *Composites Part A*, **2001**, *32*,143-172.

[52] Grigoras S, Gusev AA, Santos S, Suter UW, *Polymer*, **2002**, *43*, 489-494.

[53] Chun I, Reneker DH, Fang XY, Fong H, Deitzel J, Tan NB. *International SAMPE Symposium and Exhibition* (Proceedings), **1998**, *43*, 718-729.

[54] Dzenis YA, Wen YK, *Materials Research Society Symposium-Proceedings*, **2002**, *702*, 173-178.

[55] Wang Y, Serrano S, Santiago-Aviles JJ. *Journal of Materials Science Letters*, **2002**, *21*, 1055-1057.

[56] Berry JP, *US patent*, 4965110, **1990**.

[57] Bornat A, *US Patent*, 4689186, **1987**.

[58] Hohman MM, Shin M, Rutledge G, Brenner MP, *Physics of Fluids*, **2001**, *13*, 2221-2236.

[59] Martin GE, Cockshott ID, Fildes FJT. *US patent*, 4044404, **1977**.

[60] Martin GE, Cockshott ID, Fildes FJT. *US patent*, 4878908, **1989**.

[61] Scopelianos AG. *US patent*, 5522879, **1996**.

[62] Buchko CJ, Chen LC, Shen Y, Martin DC, *Polymer*, **1999**, *40*, 7397-7407.

[63] Buchko CJ, Slattery MJ, Kozloff KM, Martin DC, *J. Mat. Res.*, **2000**, *15*, 231-242.

[64] Buchko CJ, Kozloff KM, Martin DC, *Biomaterials*, **2001**, *22*, 1289-1300.

[65] Laurencin CT, Ambrosio AMA, Borden MD, Cooper Jr JA. *Annu. Rev. Biomed. Eng.*, **1999**, *1*, 19-46.

[66] Buchko CJ, Chen LC, Shen Y, Martin DC, *Polymer*, **1999**, *40*, 7397-7407.

[67] Fertala A, Han WB, Ko FK, *J. Biomed. Mater. Res.*, **2001**, *57*, 48-58.

[68] Huang L, McMillan RA, Apkarian RP, Pourdeyhimi B, Conticello VP, Chaikof EL, *Macromolecules*, **2000**, *33*, 2989-2997.

[69] Yoshimoto H, Shin YM, Terai H, Vacanti JP, *Biomaterials*, **2003**, *24*, 2077-2082.

19

[70] Shortkroff S, Li Y, Thornhill TS, Rutledge GC, *Abstr. Pap. Am. Chem. Soc.*, **2002**, *224*, U504.

[71] Li WJ, Tuli R, Huang XX, Laquerriere P, Tuan RS, *Biomaterials*, **2005**, *26*, 5158-5166.

[72] Pham QP, Sharma U, Mikos AG, *Biomacromolecules*, **2006**, *7*, 2796-2805.

[73] Yang F, Murugan R, Wang S, Ramakrishna S, *Biomaterials*, **2005**, *26*, 2603-2610.

[74] Badami AS, Kreke MR, Thompson MS, Riffle JS, Goldstein AS, *Biomaterials*, **2006**, *27*, 596-606.

[75] Zong X, Bien H, Chung CY, Yin L, Fang D, Hsiao BS, Chu B, Entcheva E, *Biomaterials*, **2005**, *26*, 5330-5338.

[76] Zhang Y, Ouyang H, Lim CT, Ramakrishna S, Huang ZM, *J. Biomed. Mater. Res.*, **2005**, *72B*, 156-165.

[77] Chakrapani VY, Gnanamani A, Giridev VR, Madhusoothanan M, Sekaran G, *J. Appl. Polym. Sci.*, **2012**, *125*, 3221-3227.

[78] Kim HW, Yu HS, Lee HH, *J. Biomed. Mater. Res.*, **2008**, *87A*, 25-32.

[79] Han JJ, Lazarovici P, Pomerantz C, Chen XS, Wei Y, Lelkes PI, *Biomacromolecules*, **2011**, *12*, 399-408.

[80] Cui W, Li X, Chen J, Zhou S, Weng J, *Cryst. Growth Des.*, **2008**, *8*, 4576-4582.

[81] Ma ZW, He W, Yong T, Ramakrishna S, *Tissue Eng.*, **2005**, *11*, 1149-1158.

[82] Jin HJ, Fridrikh S, Rutledge GC, Kaplan D. *Abstracts of Papers American Chemical Society*, **2002**, *224*, 408.

[83] Martindale D. *Scientific American*, **2000**, 34-36.

[84] Smith D, Reneker DH. PCT/US00/27737. **2001**.

[85] Kenawy ER, Bowlin GL, Mansfield K, Layman J, Simpson DG, Sanders EH, *Journal of Controlled Release*, **2002**, *81*, 57-64.

[86] Zussman E, Yarin AL, Weihs DA, *Experiments in Fluids*, **2002**, *33*, 315-320.

[87] Ignatious F, Baldoni JM, PCT/US01/02399, **2001**.

[88] Smith D, Reneker DH, Schreuder GH, Mello C, Sennett M, Gibson P. PCT/US00/27776, **2001**.

[89] Day M, Cooney JD, Suprunchuk T, *Text. Res. J.*, **1988**, *58*, 141-147.

[90] An SK, Barker RL, Stull JO, ASTM STP 1037. *American Society for Testing*

and Materials, **1989**, 86-101.

[91] Vogelpohl TL, *Dissertation*, University of Kentucky, **1996**.

[92] Poli T, Toniolo L, Sansonetti A, *Macromol Symp*, **2006**, *238*, 78-83.

[93] Pickett JE, Sargent JR, *Polym. Degrad. Stab.*, **2009**, *94*, 189-195.

[94] Bresee RR, Annis PA, Warnock MM, *Text. Chem. Color.*, **1994**, *26*, 17-23.

[95] Annis PA, Bresee RR, *Text. Res. J.*, **1990**, *60*, 541-548.

[96] Jorgensen GJ, Kim HM, Wendelin TJ, ASTM STP 1294. *American Society for Testing and Materials*, Pennsylvania, **1996**, 121-135.

[97] Smith D, Reneker DH, PCT/US00/27737, **2001**.

[98] Gibson P, Schreuder-Gibson H, *ACS Symposium Series*, **2006**, *918*, Oxford University Press, USA, 121.

[99] Lee S, Obendorf SK, *Text. Res. J.*, **2007**, *77*, 696-702.

[100] Schreuder-Gibson H, Gibson P, Senecal K, Sennett M, Walker J, Yeomans W, Ziegler DJ, *J. Adv. Mater.*, **2002**, *34*, 44-55.

[101] Gibson PW, Schreuder-Gibson HL, Riven D. *AIChE J*, **1999**, *45*, 190-195.

[102] Gibson PW, *J. Coated Fabrics*, **1998**, *28*, 63-67.

[103] McCreery MJ, *US Patent*, **1997**, 5607979.

[104] Speck JC, *US Patent*, **1959**, 2885305.

[105] Gibson H L, Gibson P, Senecal K, Sennett M, Walker J, Yeomans W, Ziegler D and Tsai PP, *J. Adv. Mat.*, **2002**, *34*, 44-40.

[106] Gibson P, Schreuder-Gibson HL, Rivin D, *Colloids Surf., A*, **2001**, *469*, 187-188.

[107] Gibson PW, Schreuder-Gibson HL, Rivin D, *AICHE J.*, **1999**, *45*, 190-195.

[108] Schreuder-Gibson HL, Gibson PW, Hsieh YL, *International Nonwovens Journal*, **2002**, *11*, 21-26.

[109] Lee S, Obendorf SK, *J. Appl. Polym. Sci.*, **2006**, *102*, 3430-3437.

[110] Lee S, Obendorf SK, *Fibers and Polymers*, **2007**, *8*, 501-506.

[111] Barhate RS, Loong CK, Ramakrishna S, *Journal of Membrane Science*, **2006**, *283*, 209-218.

[112] Biswas P, Wu CY, *Journal of the Air and Waste Management, Association*, **2005**, *55*, 708-746.

[113] Chen DR, Pui DYH, Kaufman SL, *Journal of Aerosol Science*, **1995**, *26*,

963-977.

[114] Ji L, Zhang X, *Nanotechnology*, **2009**, *20*, 155705.

[115] Yagi S, Nakagawa T, Matsubara E, Matsubara S, Ogawa S, Tani H, *Electrochem. Solid-State Lett.*, **2008**, *11*, E25-27.

[116] Wang L, Yu Y, Chen PC, Chen CH, *Scr. Mater.*, **2008**, *58*, 405-411.

[117] Fan Q, Whittingham MS. *Electrochem. Solid-State Lett.*, **2007**, *10*, A48-51.

[118] Ding Y, Zhang P, Long Z, Jiang Y, Huang J, Yan W, Liu G. *Mater. Lett.*, **2008**, *62*, 3410-3416.

[119] Lee K, Manesh K, Kim K, Gopalan A, *J. Nanosci. Nanotechnology*, **2009**, *9*, 417-422.

[120] Zhan SH, Li Y, Yu HB, *J. Dispersion Sci. Technol.*, **2008**, *29*, 702-708.

[121] Zhan SH, Li Y, Yu HB, *J. Dispersion Sci. Technol.*, **2008**, *29*, 823-829.

[122] Wang L, Yu Y, Chen P, Zhang D, Chen C. *J. Power Sources*, **2008**, *183*, 717-723.

[123] Barakat N, Khil M, Sheikh F, Kim H, *J. Phys. Chem. C*, **2008**, *112*, 12225-12233.

[124] Kuo J, Lee S, Hsu K, Liu S, Chou B, Fu Y. *Mater. Lett.*, **2008**, *62*, 4594-4596.

[125] Gu Y, Jian F, *J. Phys. Chem. C*, **2008**, *112*, 20176-20180.

[126] Gu YX, Chen DR, Jiao XL, Liu FF, *J. Mater. Chem.* **2007**, *17*, 1769-1775.

[127] Lu HW, Zeng W, Li YS, Fu ZW. *J. Power Sources*, **2007**, *164*, 874-879.

[128] Gu Y, Chen D, Jiao X, Liu F, *J. Mater. Chem.*, **2006**, *16*, 4361-4366.

[129] Yu N, Shao C, Liu Y, Guan H, Yang X, *J. Colloid Interface Sci.*, **2005**, *285*, 163-166.

[130] Zhao L, Zhang H, Li X, Zhao J, Zhao C, Yuan X, *J. Appl. Polym. Sci.*, **2009**, *111*, 3104-3112.

[131] Ding Y, Zhang P, Long Z, Jiang Y, Xu F, Di W, *J. Membr. Sci.*, **2009**, *329*, 56-59.

[132] Subramania A, Sundaram NK, Priya AS, Kumar GV, *J. Membr. Sci.*, **2007**, *294*, 8-15.

[133] Bansal D, Meyer B, Salomon M. *J. Power Sources*, **2008**, *178*, 848-851.

[134] Kader MA, Kwak SK, Kang SL, Ahn JH, Nah C, *Polym. Int.*, **2008**, *57*, 1199-1205.

[135] Raghavan P, Zhao X, Kim J, Manuel J, Chauhan G, Ahn J, Nah C, *Electrochim.*

Acta, **2008**, *54*, 228-234.

[136] Cho T, Sakai T, Tanase S, Kimura K, Kondo Y, Tarao T, Tanaka M, *Electrochem. Solid-State Lett.*, **2007**, *10*, A159-162.

[137] Ju Y, Park J, Jung H, Lee W, *Electrochim. Acta*, **2007**, *52*, 4841-4847.

[138] Cheruvally G, Kim JK, Choi JW, Ahn JH, Shin YJ, Manuel J, Raghavan P, Kim KW, Ahn HJ, Choi DS, Song CE, *J. Power Sources*, **2007**, *172*, 863-869.

[139] Kim C, Park SH, Lee WJ, Yang KS, *Electrochim. Acta*, **2004**, *50*, 877-881.

[140] Waters CM, Noakes TJ, Pavery I, Hitomi C, *US patent*, 5088807, **1992**.

[141] Lee SH, KumarJ, Tripathy SK, *Langmuir*, **2000**, *16*, 10482-10489.

[142] Deitzel JM, Kleinmeyer J, Tan NC, *Polymer*, **2001**, *42*, 261-272.

[143] Long YZ, Li MM, Gu C, Wan M, Duvail JL, Liu Z, Fan Z, *Prog. Polym. Sci.*, **2011**, *36*, 1415-1442.

[144] Wang X, Drew C, Lee SH, Senecal KJ, Kumar J, Samuelson LA, *Nano Lett.*, **2002**, *2*, 1273.

[145] Long Y, Chen H, Yang Y, Wang H, Yang Y, Li N, Li K, Pei J, Liu F, *Macromolecules*, **2009**, *42*, 6501.

[146] Haglund RF, Yang JL, Magruder RH, Wittig JE, Becker K, Zuhr RA, *Opt. Lett.*, **1993**, *18*, 373-375.

[147] Hu MS, Chen HL, Shen CH, Hong LS, Huang BR, *Nat. Mater.*, **2006**, *5*, 102-106.

[148] Shi W, Lu WS, Jiang L, *J. Colloid Interface Sci.*, **2009**, *340*, 291-297.

[149] Fang X, Bando Y, Liao M, Zhai T, Gautam UK, Li L, Koide Y, Golberg D, *Adv. Funct. Mater.*, **2010**, *20*, 500-508.

[150] Wang XY, Drew C, Lee SH, Senecal KJ, Kumar J, Samuelson LA, *Nano Lett.*, **2002**, *2*, 1273-1275.

[151] Heng LP, Wang XY, Dong YQ, Zhai J, Tang BZ, Wei TX, Jiang L, *Chem. Asian J.*, **2008**, *3*, 1041-1046.

[152] Wang XY, Kim YG, Drew C, Ku B C, Kumar J, Samuelson LA, *Nano Lett.*, **2004**, *4*, 331-334.

[153] Wang XY, Drew C, Lee SH, Senecal KJ, Kumar J, Samuelson LA, *Nano Lett.*, **2002**, *2*, 1273-1275.

[154] Tao SY, Li GT, Yin JX, *J. Mater. Chem.*, **2007**, *17*, 2730-2736.

[155] Patel AC, Li SX, Yuan JM, Wei Y, *Nano Lett.*, **2006**, *6*, 1042-1046.

[156] Bognitzki M, Hou H, Ishaque M, Frese T, Hellwig M, Schwarte C, *Adv. Mater.*, **2000**, *12*, 637-640.

[157] Hou HQ, Jun Z, Reuning A, Schaper A,Wendorff JH, Greiner A, *Macromolecules*, **2002**, *35*, 2429-3241.

[158] Zhang C, Yuan X, Wu L. *Eur. Polym. J.*, **2005**, *41*, 423-428.

[159] Tao J, Shivkumar S. *Mater. Lett.*, **2007**, *61*, 2325-2331.

[160] Shenoy SL, Bates WD, Frisch HL, *Polymer*, **2005**, *46*, 3372-3378.

[161] Shenoy SL, Bates WD, Wnek G, *Polymer*, **2005**, *46*, 8990-8996.

[162] Yao L, Haas TW, Guiseppi-Elie A, *Chem. Mater.*, **2003**, *15*, 1860-1867.

[163] Theron SA, Zussman E, Yarin AL. *Polymer*, **2004**, *45*, 2017-2030.

[164] Koski A, Yim K, Shivkumar S. *Mater. Lett.*, **2004**, *58*, 493-497.

[165] Lee JS, Choi KH, Ghim HD, Kim SS, Chun DH, Kim HY, Lyoo WS. *J. Appl. Polym. Sci.*, **2004**, *93*, 1638-1646.

[166] Wang C, Dong H, Hu W, Liu Y, Zhu D. *Chem. Rev.*, **2012**, *112*, 2208-2267.

[167] Chuangchote S, Fijita M, Sagawa T, Sakaguchi H, Yoshikawa S. *ACS Appl. Mater. Interfaces*, **2010**, *2*, 2995-2997.

[168] Lee SW, Lee HJ, Choi JH, Koh WG, Myoung JM, Hur JH, Park JJ, Cho JH, Jeong U. *Nano Lett.*, **2010**, *10*, 347-351.

[169] Yin K, Zhang L, Lai C, Zhong L, Smith S, Fong H, Zhu Z. *J. Mater. Chem.*, **2011**, *21*, 444-448.

[170] Kim T, Im JH, Choi HS, Yang SJ, Kim SW, Park CR. *J. Mater. Chem.*, **2011**, *21*, 14231-14239.

CHAPTER 2 Improvement of the electrospinning process of PVA via dialysis and complexation pretreatment

Abstract

The electrospinning process of polyvinyl alcohol (PVA) aqueous solutions for two samples (HS and FL) was carried out. FL solutions produced nanofibers in electrospinning process, whereas HS solutions showed poorer electrospinning process accompanying dropping and electrospraying. The analysis of the spinning solution properties indicated that the electric conductivity and viscosity of both FL and HS solutions demonstrated similar behaviors. However, the surface tensions of FL solutions were slightly decreased while the surface tension presented U-shaped curves for HS solutions with the increase of polymer concentration. The NMR spetra and DSC results implied that HS had higher degree of saponification. The metal element analysis results meant that HS contained high concentrations of calcium and aluminum ions while FL much less. The dosage of calcium chloride into FL aqueous solutions indicated that electrospinning process was significantly aggravated. The electrospinnability of HS was substantially improved both by dialysis and complexation. It was the high degree of saponification and it was intramolecular cross-linking and intermolecular cross-linking occurred between PVA chain and the metal ions that coined the abnormal behaviors in surface tension and thus deteriorated electrospinnability.

2.1 Introduction

Poly (vinyl alcohol) (PVA) is a semi-crystalline hydrophilic polymer with highly biocompatible, non-toxic, good chemical and thermal stability, and thus these prominent properties led PVA to find its wide applications. The electrospinnability and its non-woven fabric properties of PVA with different saponification degree (SD) [1], molar mass [2, 3] and pH value [4] have been investigated carefully. High saponification degree, large molar mass as well as low pH values all impeded electrospinning. Since the production of PVA is multi-step process, the monomer source, polymerization route and saponification process may give rise to PVA with

the differences in molar mass, tacticity, and metal ion impurity and so on. The effects of di or trivalent metal ions on electrospinning process haven't been paid any attention yet, however, the di- and trivalent metal ions can substantially change the viscosity, electric conductivity and surface tension of aqueous PVA solutions because PVA can physically interact with these metal ions [5]. In this work, the effects of di- and trivalent metal ions and of saponification degree were studied in details.

2.2 Experimental

2.2.1 Raw materials

PVA1750 with SD=99+%, the polymerization degree 1,750 and intrinsic viscosity 0.913, made in China (abbr. HS); PVA1600 with SD=97.5-99.5%, the polymerization degree 1,600, and the intrinsic viscosity 0.864, Fluka (abbr. FL); ethylene diamine tetraacetic acid (EDTA) and anhydrous calcium chloride, analytical grade; deionised water; regenerated cellulose dialysis bag (MWCO 10000 Dalton).

2.2.2 Preparation of solutions

PVA was dissolved into deionised water at 70 °C for 2 h. The solution was filled into a dialysis bag and dialysed with renewing fresh deionised water for every 2 h. The dialysis operation lasted for 2 days. EDTA was dissolved in water before being added to aqueous PVA solution.

2.2.3 Electrospinning conditions

The distance between needle and target Tcd=150 mm, spinning voltage=16 kV, ambient temperature=20 °C, relative humidity RH=70%. The spinning hole or spinneret was made in the following way: a glass tube was heated and drawn to get a conical tip, and the commercial polyethylene vial sampler (0.5 ml) was fixed tightly on the glass conical tip. The internal diameter of the polyethylene vial was ca.0.7 mm, and the flow rate was ca. 0.1 ml/h. Usually the electrospinning was carried out within 2 h after PVA was dissolved completely, otherwise the spinning solution would be treated with ultrasonic dispersion prior to electrospinning.

2.2.4 Characterization of solution properties and fiber morphology

The conductivity and surface tension of PVA aqueous solutions were measured by

using a conductivity meter (DDB-303A, Shanghai Leici Instruments Co. Ltd) and a surface tension meter (DW-P503-4AC), respectively, at 20 °C. The viscosities of PVA aqueous solutions were measured on a coaxial cylinder viscometer (NDJ-79, Shanghai Changji Geological Instruments Co. Ltd) at 20 °C. The melting point of raw PVA was measured with Perkin-Elmer (DSC-7) under nitrogen flow with the flow rate 40 ml/min and the heating rate 10 °C/min. The morphology of electrospun fibers was observed on a scanning electron microscope (SEM) (HITA-CHI S-570) after gold coating. The ^{1}H NMR spectra were aquired with Bruker AV-400 NMR spectrometer, D_2O as solvent and at amibent temperature. A weighted PVA sample was burned in a Muffle furnace at 600 °C for 2 h, and the residue was dissolved in dilute nitric acid. The solution was used for measuring the concentrations of metal ions with Plasma Emission Spectrometry (PLA-SPECI).

2.3 Results and discussion

2.3.1 Electrospinning of PVA aqueous solutions

HS solutions at the different PVA concentrations ranging between 7 and 9 w/v% mainly showed electrospraying rather than electrospinning, no continuous fibers were formed even at all PVA concentrations with solution dropping at the tip of needle. FL solutions indicated the steady electrospinning with no dropping, and smooth and uniform nanofibers were produced. Koski et al concluded that the product of polymer intrinsic viscosity and polymer concentration ($[\eta]C$) controlled electrospinnabiliy, and the minimum value would be 5 from electrospraying to electrospining for PVA. In our case, HS had polymerization degree was 1,750 and minimum concentration 7 w/v %, the value of $[\eta]C$ was ca. 5. It seemed the theory didn't work well for sample HS. Shenoy et al. [6] thought that the event of chain entanglements dominated electrospinnability, and suggested that the minimum number of chain entanglement points for fiber initiation be 2. The repeating units of PVA for the event of chain entanglement were assumed to be the same as polyethylene since intramolecular and intermolec-ular hydrogen bonding of PVA might offset the bulky effect of hydroxyl group, and thus the molar mass of chain entanglement for PVA was 1,964. The volume fraction 8_p for PVA concentration 7 w/v% was ca 0.0526. The number of chain entanglement points (Ne) in PVA 7 w/v% solution 2.06. Shenoy's theory also implied that 7 w/v% concentration of PVA

should be the minimum concentration for the electrospinning. Unfortunately it fell again. In addition, Yao et al. [7] pointed that it was difficult to get the PVA concentration of 10 wt % with molar mass 115,000 to be electrospun. Actually in the Yao's system, the values of $[\eta]C$ and Ne were calculated to be 9.8 and 4.31, respectively, the flat electrospun fiber can be resulted in the light of Shenoy's theory if it is possible to be spun; and the value 4.31 of Ne would mean that the solution located at very high concentration ranges with $[\eta]$ proportional to $M_w^{3.4}$. Thus the difficult electrospinning originated from a very high polymer concentration and high molar mass. It seemed hard to explain electrospinning clearly only based on the solution theories for our case, and the microstructure of PVA and the properties of solutions would be investigated accordingly.
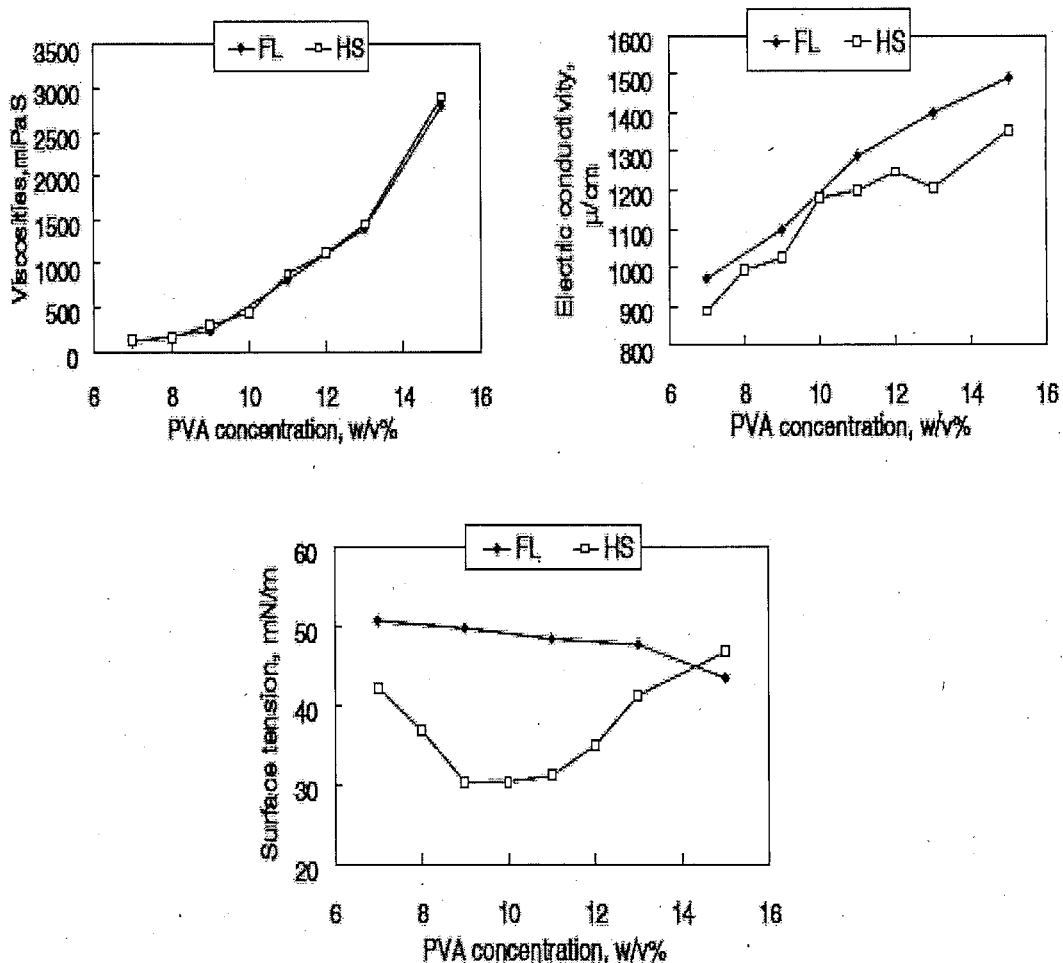
Figure 2.1 Solution properties f PVA aqueous solutions

Figure 2.1 give the viscosity, conductivity and surface tension of the two PVA solutions. The viscosity and electric conductivity of the two solutions show similar

tendencies with PVA concentrations, whereas the surface tension of HS presented abnormal behavior as comparison with those of FL. Generally speaking, the surface tension would be lessened and then leveled off and the viscosity and the conductivity would be increased monotonically with the increase of PVA concentrations, and the electrospinnability of PVA solutions would consequently be improved, namely from electrospraying to electrospinning, which was implied in the references 2 and 6, and this would be also conformed in our work for FL.

Table 2.1 Content of di-or trivalent metal ions of three PVA raw materials (ppm)

Elements	Cr	Cu	Fe	Mg	Mn	Ti	Zn	Al	Ca	Equivalence in solution, mM
HS	0.13	5.3	10	2.3	1.8	1.4	0.43	53	48	0.64
FL	/	/	/	0.1	/	/	/	10	22	0.15

● metal ions   ——— macromolecule
         — water molecule
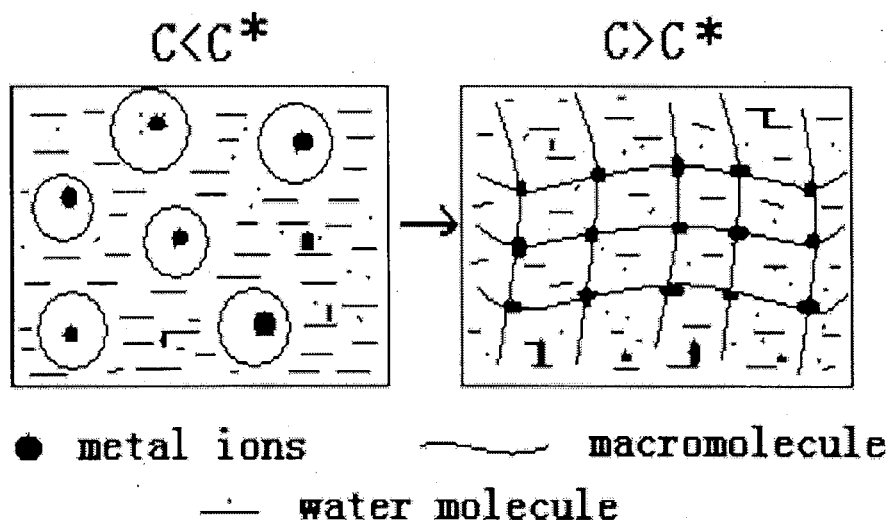
Figure 2.2 Illustration of di-and tri-valent metal ions interaction with polymer chains

Table 2.1 lists the contents of some di- and tri-valent metal ions in PVA raw materials. FL contained trace amounts of di- and trivalent metal ions, while HS had diversified metal ions with high concentrations. The equivalent number was calculated by the product of mole number and usual valence of metal ions, and then converted into the value corresponding to 7 w/v% concentration. The equivalence

number of FL was much smaller than that of HS. PVA chains may interact with these trace amounts of di- and trivalent metal ions and form physical cross-links, and this would multiply viscosity and turn surface tension upside down. The U-shaped surface tension for sample HS was understood as follows: at low polymer concentrations, metal ions caused intramolecular cross-links and made PVA chains compacted and led surface tension of the solution to be increased; at high polymer concentrations, the metal ions caused intermolecular cross-links and the resultant physical gels were fully filled in the whole vessel. When the surface tension was measured only by breaking the gels, the surface tension of similar virgin water was obtained, and hence the high surface tension was picked coincidently. This explanation was schematically presented in Figure 2.2. The intramolecular and intermolecular crosslinking effects due to higher valent metal ions substantially varied the configuration of macromolecular chains, namely the dissolution behaviour of PVA, and thus the surface tension of PVA aqueous solution. Actually Yao et al improved the electrospinning of PVA with high molecular weight by addition of the surfactant Triton X-100 [7]. At low polymer concentrations, intramolecular cross-linking effects reduced the chance of interchain contacts and theelectrospraying was resulted while with solution dropping at the tip of needle. At the high concentrations of PVA, of course the higher of metal ion content, intermolecular cross-linkings due to high valence metal ions made the solution viscosity become high but much brittle, then the solution was difficult to go through the needle, and hence electrospraying and ocassionally few pieces of flat filaments were got while with solution dropping at the tip of needle. Accordingly, it is the presence of high concentrations of di- and tri-valent metal ions that cause the abnormal surface tension behaviours and further the electrospinnability of HS solutions to be deteriorated. Zhang et al claimed that the relatively high saponification degree, especially with saponification degree over 99%, might also impair electrospinnability of PVA. Obviously this may be due to stronger intramolecular and intermolecular hydrogen bondings at higher saponification degrees. The melting points of FL and HS raw materials were 223.4 and 232.3 °C, respectively and the values implied that the SD of FL would be lower than that of HS because the residual acetyl groups in PVA chain damaged its regularity and then hindered crystallization and further diminished crystallite sizes. Figure 2.3 shows the

proton NMR spectra for the two samples. The peak attribution is tabulated in Table 2.2 [8]. The adsorption in the areas of 1.909-1.991 for FL were much stronger than that of HS, and this implied that more acetyl groups were still appended in PVA chains for FL than for HS. Therefore, the higher the saponification degree, the more difficult the electrospinning. This finding complied with Zhang's conclusion. We will further testify the effect of saponification degree in our ongoing project.
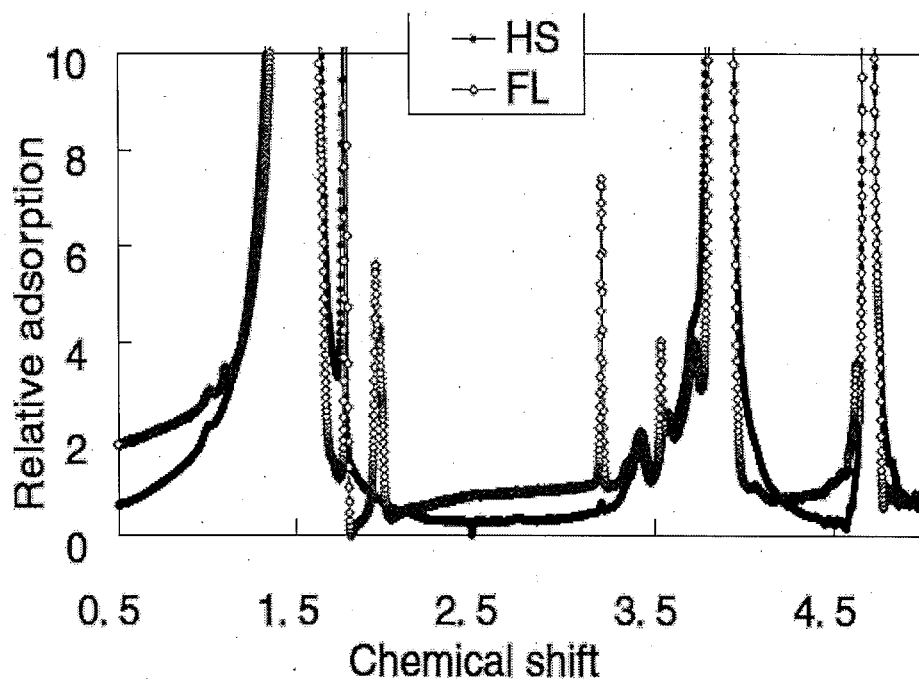
Figure 2.3 ^{1}H NMR spectra for two samples

Table 2-2 The peak assignment from ^{1}H NMR spectra [8]

H source	OH from water and PVA	Methine —CH—	Methyl from methanol[a]	Residual acetyl groups (CH$_3$CO–)	Sodium acetate[b] (CH$_3$COONa)	Methylene from chain (–CH$_2$–)
position	4.702	3.888	3.205	1.905–1.991	1.775	1.457–1.560

[a] Methyl group came from residual solvent methanol in PVA particles.
[b] Sodium acetate was a byproduct during saponification.

2.3.2 Electrospinning process after dialysis and complexation
treatment
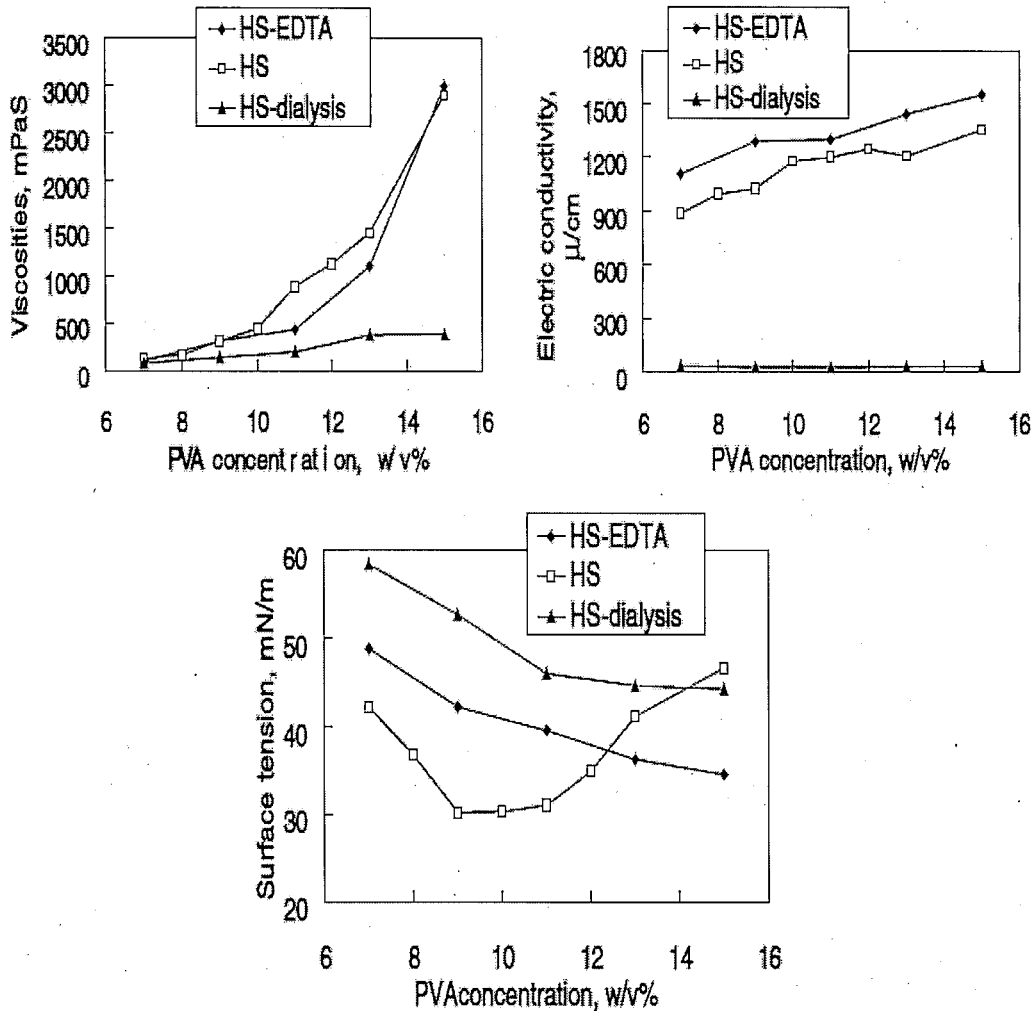
Figure 2.4 Solution properties of all sample HS

Figure 2.4 give the solution properties of virgin HS solutionsand of HS solutions after EDTA complexation and dialysis pretreatments. After the complexation with EDTA, the viscosities of PVA solutions were somewhat reduced only at the concentrations ca 10-14 w/v% in comparison to untreated PVA solutions, whereas the surface tension behaviors did change substantially and dwindled monotonically with the increase of PVA concentration. After the dialysis treatment, the electric conductivity markedly fell down, while the viscosities diminished significantly possibly because the all metal ions such as sodium, calcium and aluminum ions were

got rid of by flushing water and the interaction between metal ions and the hydroxyl groups of PVA chains were thereby removed. This can confirm that the metal ions did produce physical cross-links between polymer chains. The surface tension also gradually decreased with PVA. The electrospinnability of treated HS samples are dispalyed in Figure 2.5, where the polymer concentrations were all 7 w/v%. The untreated HS solution only got unshaped nano-particles, the dialysed and the complexation HS solutions both showed excellent spinnability. As also can be seen from Figure 2.5, the diameters of filaments after dialysis were larger than those of filaments after complexation. The reason was that, the removal of metal ions from solutions reduced the splitting of filament during spinning due to the reduction of electric force, on the other hand, got the increase of surface tension of solutions and thereby the increase of filament diameter.
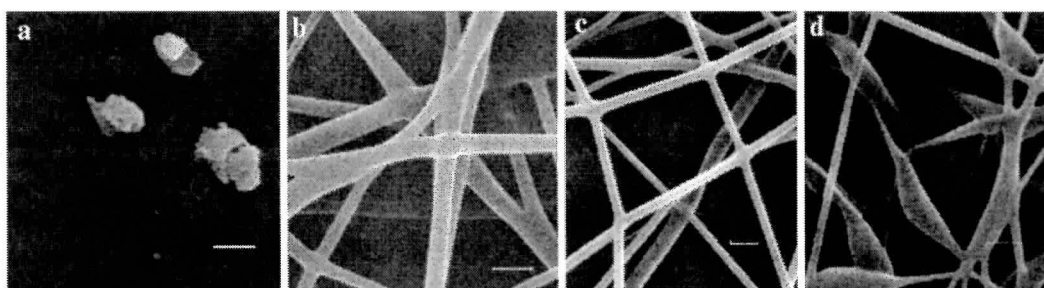
Figure 2.5 SEM images of different PVA fiber morphology (a HS, b HS after dialysis, c HS after complexation with EDTA, d FL after the dosaging of CaCl$_2$, scale bar: 600 nm)

2.3.3 Electrospinning process of FL solutions after the addition of divalent metal ions

In order to testify the negative effect of divalent metal ions on electrospinning, the anhydrous calcium chloride, the equivalence number 3.6 mM was directly added into FL solution, and the solution was spun under the same conditions as the undosaged conterpart. The image d in Figure 2.5 evidences that the calcium ions did aggravate PVA electrospinnability, and only the fiber with spindles present, instead of smooth and uniform fiber, was obtained.

2.4 Conclusions

(1) Di-and trivalent metal ions interacted with the hydroxyl groups of PVA especially at high saponification degree and produced intramolecular and intermolecular physical cross-links and thus deteriorated electrospinning process.

(2) Removal of various metal ions by using dialysis substantially changed solution properties and remarkably improved electrospinning process.

(3) Complexation with EDTA of di-and tri-valent metal ions mainly changed surface tension tendency and this markedly enhanced PVA electrospinning process.

References

[1] Zhang C, Yuan X, Wu L, sheng J. *J. Euro. Polym.*, **2005**, *41*, 423-432.

[2] Koski A, Yim K, Shivkumar S. *Mater. Lett.*, **2004**, *58*, 493-497.

[3] Lee JS, Chol KH, Ghim H-D. *J. Appl. Polym. Sci.*, **2004**, *93*, 1638-1646.

[4] Son WK, Youk JH, Lee T-S. *Mater. Lett.*, **2005**, *59*,1571-1575.

[5] Xu FL, Li YB, Wang XJ. *Funct. Mater.*, **2004**, *35*, 509-512.

[6]Shenoy SL, Bates WD, Frisch HL. *Polymer*, **2005**, *46*, 3372-3384.

[7] Yao L, Haas TW, Guiseppi-Elie A. *Chem. Mater.*, **2003**, *15*, 1860-1864.

[8] Dean JA. Lange's chemistry handbook, 15th edn, Chap 7 Section 7.7 Nuclear Magnetic Resonance.

CHAPTER 3: Effect of interaction between hydroxyl group and high valence metal ion impurity on the electrospinninng process of PVAs

Abstract

The production of superfine polyvinyl alcohol (PVA) fiber is usually much difficult by using the routine spinning, whereas electrospinning is a viable technique since the mechanism of fiber formation was different. In this paper, the effects of solution properties in terms of the residual acetyl group and high valence metal ion impurity of PVA on electrospinning were carefully investigated. Both the solution viscosity and the surface tension tendencies with PVA concentration indicated that there existed strong physico-chemical interaction besides concentration and molar mass factors. NMR spectra and DSC thermographs indirectly showed that the devoid acetyl group of PVA would promote the physical gelation and the formation of hydrogen bondings, and the physical crosslinking occurred at high saponification degrees in the presence of high valence metal ion impurity. All the interactions aggravated the electrospinnability. Nevertheless, both removal of high valence metal ion impurity and the selection of PVA with low saponification degrees would be always accessible routes to ensure the PVA electrospinning.

3. 1 Introductionon

Polyvinyl alcohol is a semi-crystalline hydrophilic polymer with excellent biodegradability, physico-chemical properties and thermal stability. The prominent properties make it attractive for a variety of applications such as film, fiber and coatings in industry. With nanotechnology and nanostructure materials widely being recognized, the electrospinning of nanofibers or ultrafine fibers from polyvinyl alcohol and its mixtures has received a great deal of attention in the past decade.

The effects of spinning conditions, polymer microstructure, and additives on the PVA electrospinnability have been investigated intensively. Zhang et al. comprehensively studied the effects of electric voltage, tip-target distance, flow rate, and cosolvent ethanol on fiber morphology [1]. Tao and Shivkumar found that, the

structural regimes for beads, beaded fibers, complete fibers and flat ribbons were mapped with the product of intrinsic viscosity and polymer concentration from 8.1 to 22.1; the onset of significant polymer chain entanglements accompanied the development of a stable fiber structure [2]. Shenoy et al thought that chain entanglement numbers in the nonspecific polymer-polymer interaction solution for both fiber initiation and complete formation should be larger than 2.5 and 3.5, respectively [3]. In their successive work, they further proposed that the entanglement numbers for the two events be much smaller for the polymer solutions with physical gelation occurring [4]. In addition, both Zhang [1] and Yao [5] found that it was very difficult to prepare ultrafine fibers for the fully hydrolyzed PVA with high molar mass. In fact, saponification degree of PVA will also switch electrospinning owing to the variation of physical gelation and hydrogen bonding interaction. Therefore, the polymer chain entanglement, the physical gelation and the hydrogen bonding interaction will strongly dominate the electrospinnability and electrospinning behavior.

Son et al thought that the pH value strongly affected the PVA electrospinnability and fiber morphology possibly due to protonation with saponification degree 99.7%[6]. The average fiber diameter and morphology of the chitosan polyvinyl alcohol blend much depended on the chitosan content and the two polymer concentrations [7]. The bovine serum albumin, manganese acetate and calcium phosphate were blended respectively with aqueous PVA solution to study electrospinnability and to prepare functional materials [1, 8, 9]. Copper/PVA nanocables were produced via the electrospinning of mixture solutions of PVA, copper chloride, sodium hydrogen sulfite and hydrazine hydrate [10]. It is well-known that high valence metal ions, chitosan and protein in aqueous PVA solutions will interact with hydroxyl group, and the crosslinking structure and hydrogen bondings can thus be formed. This can change the electrospinning behaviour simply due to the increase of electrospinning solution viscosity. We were wondering how and to which extent the electrospinnability was affected in the presence of divalent metal ions? Up to now, the effect of high valence metal ion impurity on the electrospinning of PVA hasn't attracted many interests. We briefly reported electrospinnability of PVA in the presence of high valence metal ion impurity [11]. In this work, the inter-relationship between metal ions and high

saponification degree on electrospinning were further studied in detail.

3.2 Experimental

3.2.1 Raw materials

Five commercial PVA products were used, and they were HS1799, GW1999, BY1799, FL1699 and BY1788. In the four Arabic numerals, the former two numbers indicated polymerization degree, for instance, 17 implied polymerization degree of 1700; the latter two saponification degree (SD), 99 meant SD 99%.

3.2.2 Electrospinning conditions

PVA was firstly dissolved into deionised water at 70 °C for 2 h. The spinneret tip-target distance was 130 mm, spinning voltage 16 kV, ambient temperature 20 °C, relative humidity ca.70 %. The spinning spinneret was made in the following way: a glass tube was heated and melt drawn to get a conical tip, and the commercial polyethylene vial sampler (0.5 ml) was fixed tightly on the glass conical tip. The internal diameter of the polyethylene vial was ca.0.7 mm, and the flow rate was ca. 0.1 ml/h, measured with syringe pump. Usually the electrospinning was carried out within 2 h after PVA was dissolved completely, otherwise the spinning solution would be treated with ultrasonic dispersion prior to electrospinning.

3.2.3 Characterization of solution properties and fiber morphology

The electric conductivity and surface tension of PVA aqueous solutions were measured by using a conductivity meter (DDB-303A, Shanghai Leici Instruments Co. Ltd) and a surface tension meter (DW-P503-4AC), respectively, at 20 °C. The viscosity of PVA aqueous solutions was measured on a coaxial cylinder viscometer (NDJ-79, Shanghai Changji Geological Instruments Co. Ltd) at 20 °C.

The morphology of electrospun fibers was observed on a scanning electron microscope (SEM) (HITACHI S-570) after gold coating. A weighted PVA sample was burned in a Muffle furnace at 600 °C for 2 h, and the residue was dissolved in dilute nitric acid. The acidic solution was used for measuring the concentrations of metal ions with Plasma Emission Spectrometry (PLA-SPECI). The 1H NMR spectra were acquired with Bruker AV-400 NMR spectrometer, D_2O as a solvent. The measurement was carried out at ambient temperature. The thermograph of PVA

raw materials was acquired with Perkin-Elmer (DSC-7) under nitrogen flow with the flow rate 40 ml/min and the heating rate 10 °C /min.

3.3 Results and discussion

3.3.1 Electrospinning process

The electrospinnability can be judged in the light of three different features, the stability of liquid drop hanged at the spinneret tip, the continuity of spinning process and the defects free fibers. As shown in Figure 3.1, there were only particles produced at four different PVA concentrations, and no fibers but particles appeared for the sample HS1799. In fact, during spinning process, no stable liquid drops hanged at the spinneret tip. Similar result was obtained for GW1999. Electrospraying happened again at low PVA concentrations whereas a few filaments really appeared for the sample BY1799 at high PVA concentrations as indicated in Figure 3.2.
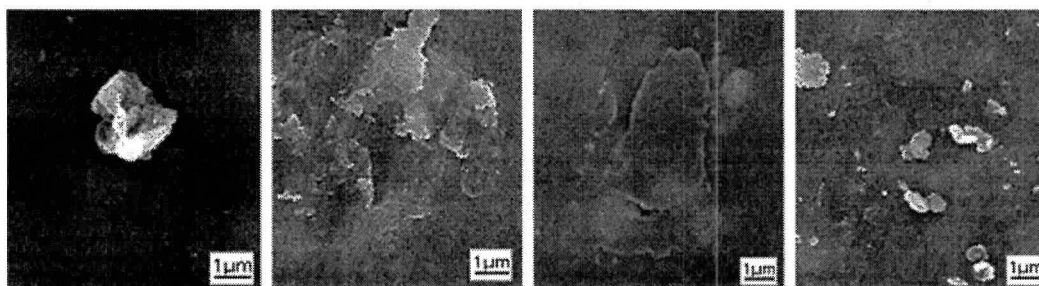
Figure 3.1 SEM images of electrosprayed deposits from HS1799 (Notation for each panel based on the order from left to right: 7, 9, 11, and 13 w/v %).
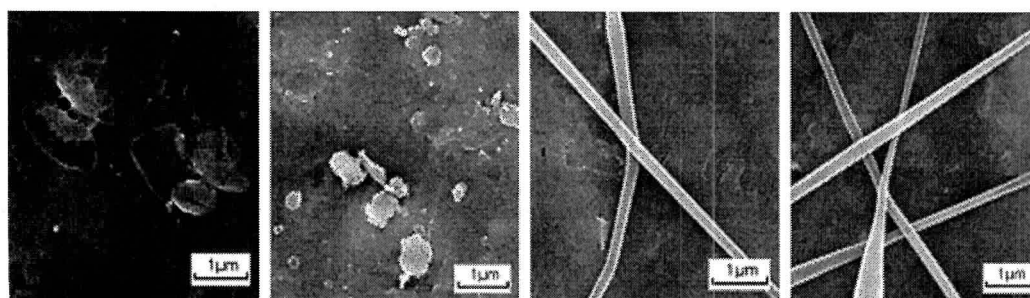
Figure 3.2 SEM images of electrospun particles and fibers from BY1799 (Notation for each panel based on the order from left to right: 7, 9, 11, and 13 w/v %).
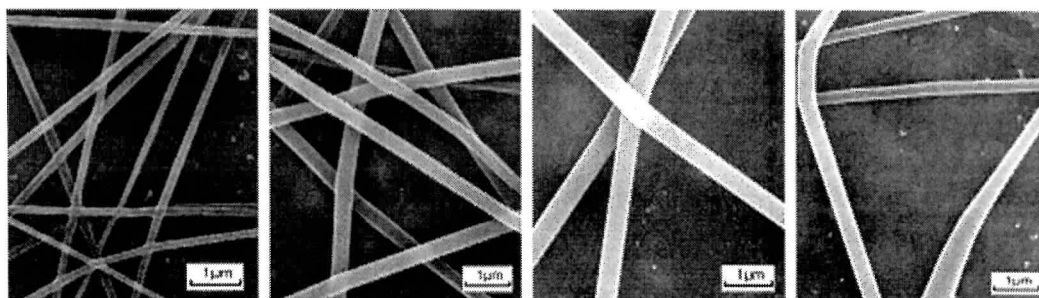
Figure 3.3 SEM images of electrospun fibers from FL1699 (Notation for each panel based on the order from left to right: 7, 9, 11, and 13 w/v %).

As shown in Figs 3.3 and 3.4, at all four PVA concentrations, really ultrafine fibers are presented. The diameters of the fibers for the low concentration PVA solutions were generally small in comparison to those at high concentrations. There existed adhesions at the fiber junction points for the sample BY1788, while not the case for the sample FL1699. The reason was that, the sample BY1788 had low saponification degree, and the PVA came up with rather good cold water solubility and namely the water retention ability was strong for BY1788. Conclusively, FL1699 displayed excellent electrospinnability, and so did BY1788. GW1999 and HS1799 really gave us disappointed results. Can we only attribute the good electrospinnability to a low polymer molar mass and a low saponification degree?
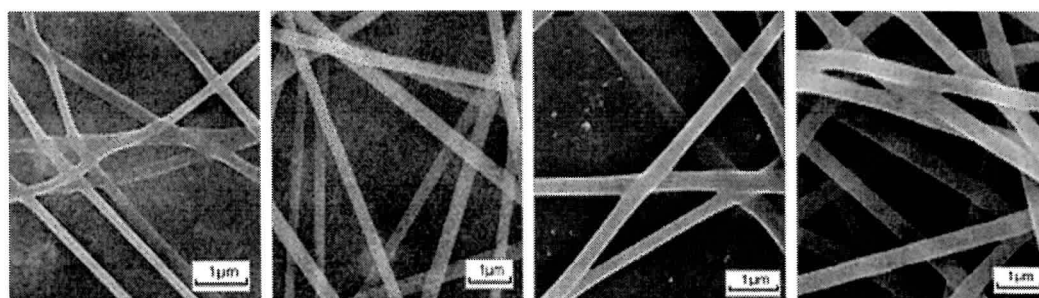
Figure 3.4 SEM images of electrospun fibers from BY1788 (Notation for each panel based on the order from left to right: 7, 9, 11, and 13 w/v %).

3.3.2 PVA Solution properties
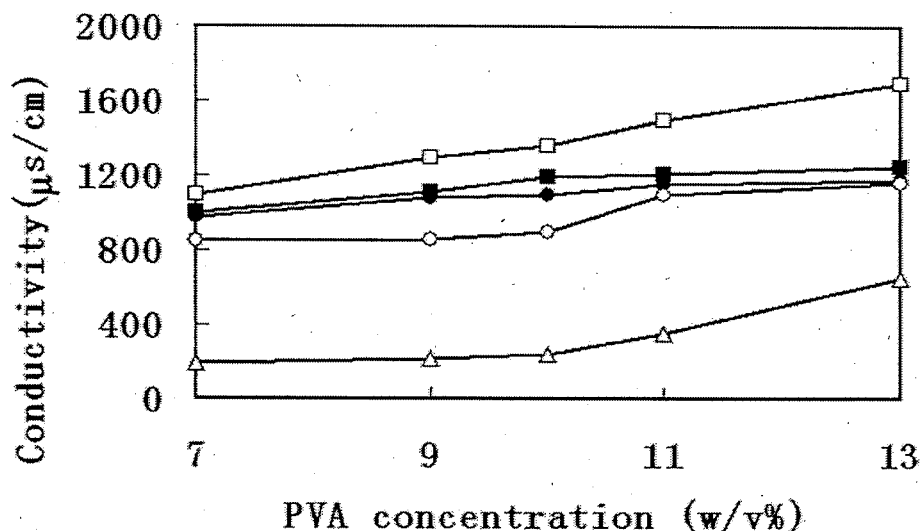
Figure 3.5 Electric conductivities of PVA aqueous solutions (●HS1799, □ GW1999, ■ BY1799, △ FL1699, ○BY1788).

Essentially the electrospinning process was controlled by mutually balancing the three forces, electric field force, cohesive force and surface tension. In reality, the electrospinnability of polymers could be indicated by the solution properties including electric conductivity, viscosity and surface tension. The electric conductivity of 5 kinds of PVA products is given in Figure 3.5. The conductivity almost linearly increased with PVA concentration, and this feature might imply that electric conductive components came from the solute PVA. Main electric conductive components should be sodium acetate, the byproduct in the hydrolysis of polyvinyl acetate. The contents of conductive components for FL1699 and BY1788 were less than those of the other three. A high conductivity caused the increase of the electric field force and thus positive charge repulsion was strengthened and the electrospun jets would be torn intensively, at worst only PVA spots were deposited on the target collector and finally a poor electrospinnability occurred.
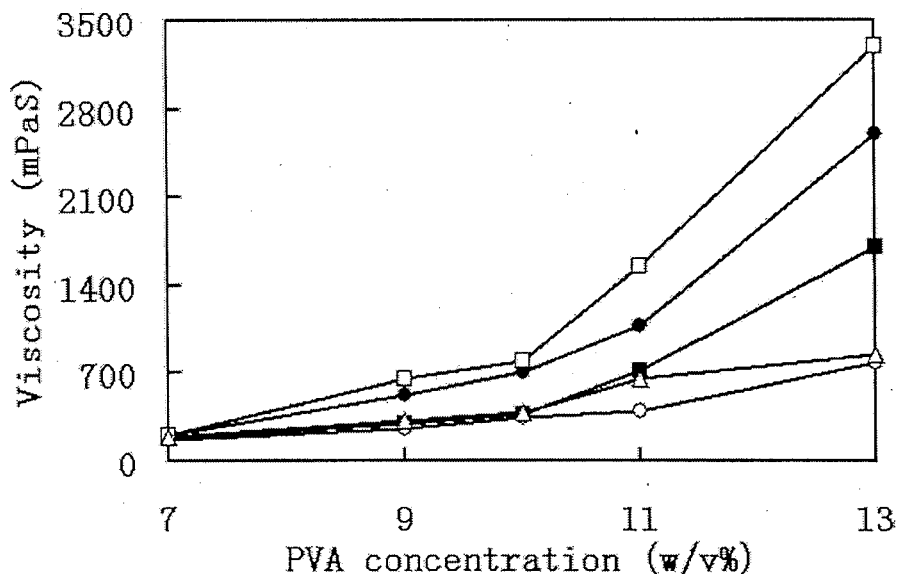
Figure 3.6 Viscosity behaviors of PVA aqueous solutions (●HS1799, □ GW1999, ■ BY1799, △ FL1699, ○ BY1788).

As indicated in Figure 3.6, BY1788 and FL1699 presented almost linear relationship of viscosity in the whole PVA concentration range. Both low polymerization degree and low saponification degree favored solubility in water. The linear relationship might be interpreted as the solutions stayed in dilute solution regime, namely, there were no polymer chain overlaps happened for the two samples. Theoretically this kind of polymer solution can't expect to give any trace of filaments [3]. Nevertheless, since PVA possesses plenty of hydroxyl groups and they will form strong hydrogen bondings, which was explained well by Shenoy et al [4], and this interaction exceptionally acted as polymer chain entanglements and then promoted fiber initiation. HS1799, GW1999 and BY1799 all showed linear relationship at the concentrations lower than 10 w/v%, and the nonlinear and upturn tendency appeared at the concentrations over 10 w/v%. The viscosity upturn behaviour implied that the polymer solution experienced transition from the dilute region to semi-dilute region, and polymer chains started to overlap, and finally polymer chain entanglements would naturally be produced. Fortunately the sample BY1799 did verify the idea while GW1999 and HS1799 didn't. It seemed that too much chemical and physical interaction violently elevated solution viscosity and caused the solutions not to be electrospun. The differences in the upturn tendencies would be caused hydrogen bondings, physical gelation and crosslinking besides the concentration and molar mass factors.
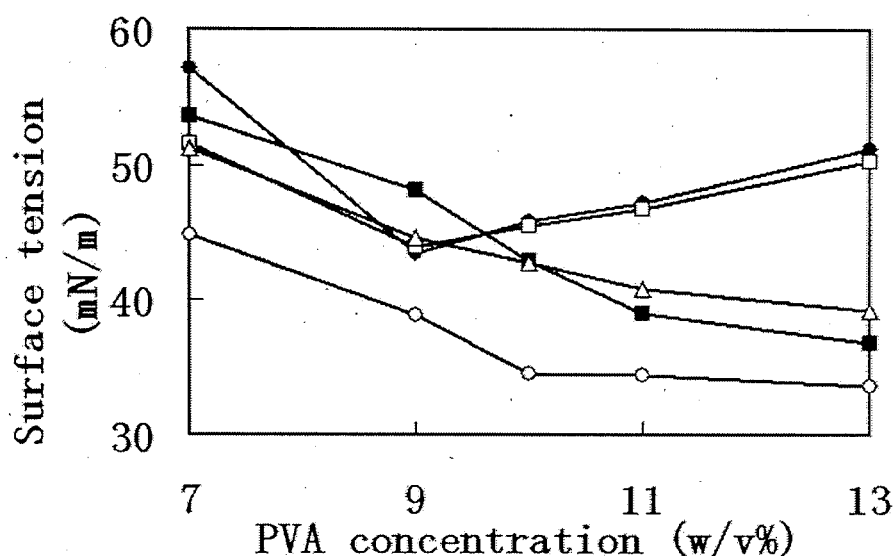
Figure 3.7 Surface tensions of PVA aqueous solutions (•HS1799, □ GW1999, ■ BY1799, △ FL1699, ○ BY1788).

The relationship between surface tension and PVA concentration appears in Figure 3.7, which didn't show similar trends as in Figures 3.5 and 3.6. The surface tensions of the samples FL1699, HS1788 and BY1799 were expectedly decreased with the increase of PVA concentration. In this case, PVA behaved itself as a surfactant, the increase of surfactant resulted in the decrease of surface tension of the solution, possibly the dissolution of PVA in water reduced the enrichment of water molecule on the solution surface due to the physical replacement of polyvinyl alcohol macromolecule. The diminution tendency of surface tension seemed an accurate signpost of PVA electropinnability. However, why the surface tension was increased when the PVA concentrations were over 9 w/v% for the samples HS1799 and GW1999? When the viscosity behaviour as shown in Figure 3.6 was taken into consideration, we could confirm that PVA chain did form strong interchain interaction, such as hydrogen bonding. This inversely lowered the phenomenological solubility of PVA and finally the surface tension was increased with PVA concentration. We may imagine that, at high PVA concentrations, the formation of physical gel due to hydrogen bondings gradually spread over the whole vessel, and the surface tensions of PVA aqueous solution were sampled only by breaking the PVA gel and then the surface tension close to the value of pure water was acquired. The formation of PVA gel may mutually comply with the high viscosity for the samples HS1799 and GW1999.

3.3.3 Macromolecular structure

The proton NMR spectra of five PVA aqueous solutions are given in Figure 3.8, and the peak assignments are listed in Table 3.1. The resonance peak for residual acetyl group was magnified in the center part in Figure 3.8. As named, BY1788 really contained most amount of acetyl groups and FL1699 medium, while there were almost no acetyl groups presented in the samples of GW1999, HS1799 and BY1799. Naturally BY1788 and FL1699 would produce less chemical and physical interaction, and their viscosity and surface tension were consequently small, and vice versa for the other three. This may also symbolize the electrospinnability of PVA.
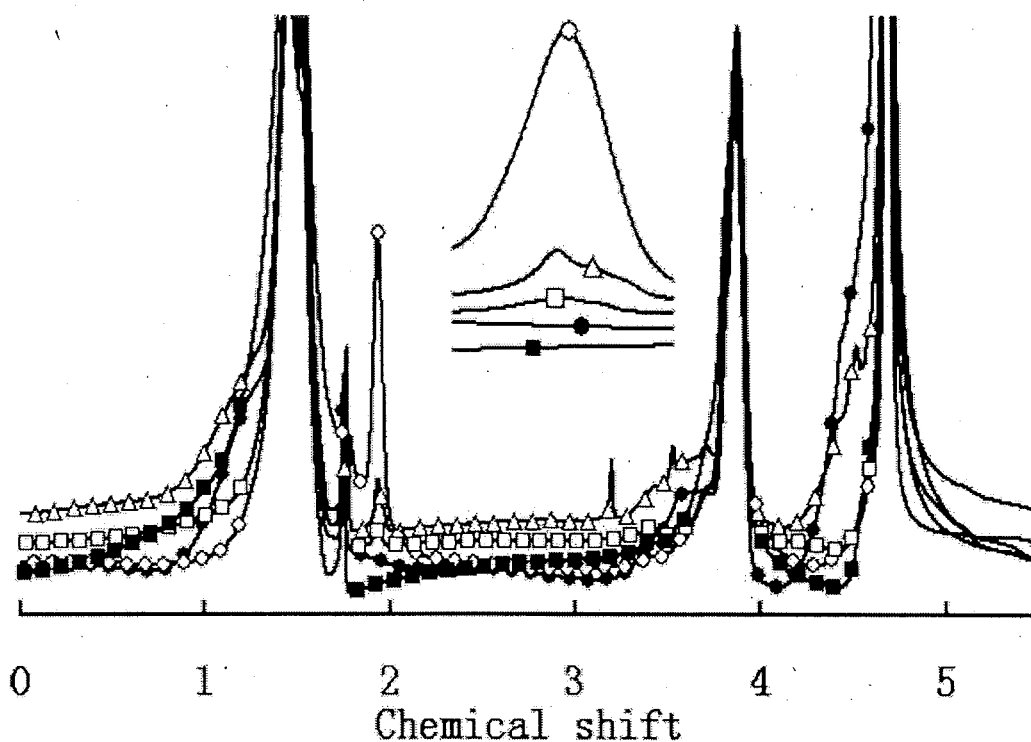
Figure 3.8 ^{1}H NMR spectra of PVA in D_2O (●HS1799, □ GW1999, ■ BY1799, △ FL1699, o BY1788).

Table 3.1 The peak assignment from 1H NMR spectra

H source	OH from water and PVA	Methine –CH–	Methyl from methanol[a]	Residual acetyl groups (CH$_3$CO–)	Sodium acetate[b] (CH$_3$COONa)	Methylene from chain (–CH$_2$–)
position	4.702	3.888	3.205	1.905–1.991	1.775	1.457–1.560

[a] Methyl group came from residual solvent methanol in PVA particles.
[b] Sodium acetate was a byproduct during saponification.

Figure 3.9 shows the thermographs of five PVA raw materials. As expected, BY1788 and FL1699 possessed the low melting temperatures ca. 197°C and 218°C respectively, whereas BY1799, GW1999 and HS1799 gave the high melting temperatures ca 222 °C, 228°C and 231 °C respectively. The residual acetyl groups in PVA chain damaged its regularity and crystallization process was hindered, and thus small crystals were resulted, and the melting temperatures of the crystals were reduced. The reduction of melting temperature complied with the analysis of content of residual acetyl group in Figure 3.8. In addition, as indicated with black arrows in Figure 3.9, HS1799 and GW1999 gave extra shoulder peak at low temperatures and were expected to form some paracrystallites in aqueous solution, and thus the existence of the crystalline states as physical gels may deteriorate electrospinnability. Conclusively, the tiny discrepancy in saponification degree induced remarkable change in crystallinity and electrospinnability.

We were wondering whether the GW1999 and HS1799 couldn't be electrospun for ever and whether hydrogen bonding and physical gelation were the only two reasons to jeopardize the electrospinnability.

3.3.4 High valence Metal ion impurity
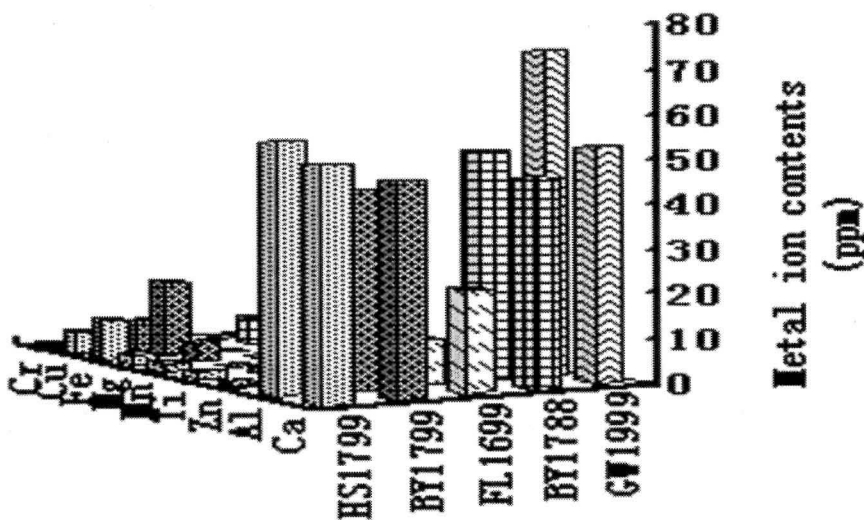
Figure 3.10 Contents of higher metal ion impurity

Figure 3.10 depicts the major divalent and trivalent metal ion contaminates in five PVA raw materials. As we can see that, calcium, aluminum and iron ions were main impurities. The sample FL1699 contained least and GW1999 most abundant while the other three showed more or less similar situations. As shown in Figs 3.1 to 3.4, the presence of high valence metal ions affected the electrospinnability possibly by forming physical crosslinking between high valence metal ion and hydroxyl group via switching viscosity and surface tension behaviors.
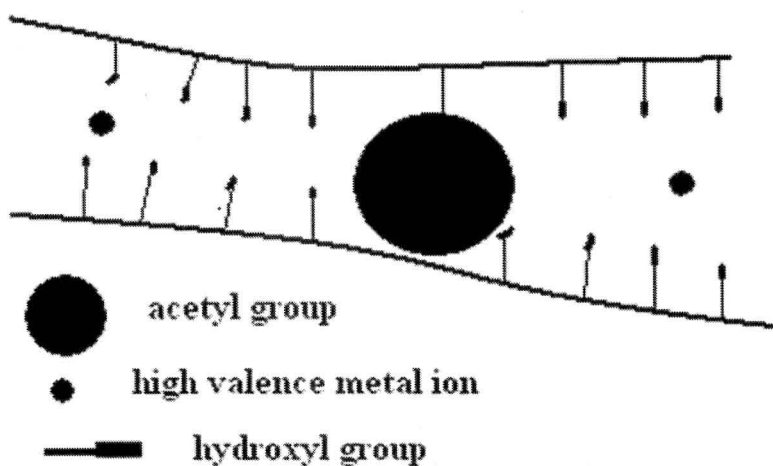
Figure 3.11 Hindrance of physical cross-linking due to the bulky acetyl group between hydroxyl group and metal ions.

The complexation process between high valence metal ion and hydroxyl group would be concentration dependent. At low PVA concentrations or in the dilute solution region, polymer chains dispersed in solution at the molecular level and no polymer chain contact event happened, and thus the complexation took place via intrachain mode. At high PVA concentrations or in the semidilute or even concentrated solution region, polymer chains would be crowded into the whole vessel, and thus the complexation occurred via interchain mode. The two interaction modes produced physical crosslinkings with opposite viscosity behaviour, namely, the lower solution viscosity was produced at low PVA concentration, and vice verse. This would deteriorate the electrospinnability of PVA samples with high saponification degree. In our previous papers[13, 14, 15], the sample HS1799 also showed pretty good electrospinnability after its solutions were dialyzed or complexed with ethylene diamine tetraacid or polyvinyl pyrrolidone or added with cosolvent acetic acid. Conclusively, high valence metal ions were thought to fortify the physical crosslinking at high saponification degree as well. Nevertheless, the residual bulky acetyl groups would prevent hydroxyl groups from forming physical crosslinking and hydrogen bonding with high valence metal ions and with other hydroxyl groups. The hindrance manner of the residual acetyl groups is schematically given in Figure 3.11. That's why the presence of large amount of metal ions didn't disturb the electrospinnability of BY1788.

3.4 Conclusions

1. The physical gelation and physical cross-linking with high valence metal ions for the fully hydrolyzed PVAs switched the solution viscosity behavior and surface tension behaviors and thus spoiled electrospinning process.

2. Both the removal of high valence metal ions and the selection of PVA with lower saponification degree were always viable routes to ensure electrospinning process.

References

[1] Zhang C, Yuan X, Wu L. *Eur. Polym. J.*, **2005**, *41*, 423-432.

[2] Tao J, Shivkumar S. *Mater. Lett.*, **2007**, *61*, 2325-2328.

[3] Shenoy SL, Bates WD, Frisch HL, *Polymer*, **2005**, *46*, 3372-3384.

[4] Shenoy SL, Bates WD, Wnek G, *Polymer*, **2005**, *46*, 8990-9004.

[5] Yao L, Haas TW, Guiseppi-Elie A, *Chem. Mater.*, **2003**, *15*, 1860-1864.

[6] Son WK, Youk JH, Lee, TS, *Mater. Lett.*, **2005**, *59*,1571-1575.

[7] Jia YT, Gong J, Gu XH, *Carbohydr. Polym.*, **2007**, *67*, 403-409.

[8] Yu N, Shao C, Liu Y. *J. Colloid. Interface. Sci.*, **2005**, *285*, 163-166.

[9] Dai X, Shivkumar S, *Mater. Lett.*, **2007**, *61*, 2735-2738.

[10] Li Z, Huang H, Wang C, *Macromol. Rapid. Commun.*, **2006**, *27*, 152-155.

[11] Zhu XS, Gao Q, Xu DT, *J. Polym. Res.*, **2007**, *14*, 277-282.

[12] Dean JA, Lange's chemistry handbook, 15th edn, Chap 7 Section 7.7 Nuclear
    Magnetic Resonance.

[13] Xu Y, Zhu XS, Gao Q, *J. Soochow. University (Eng. Sci. Edn)*, **2007**, *27*, 39-42.

[14] Gao Q, Zhu XS.; Xu Y, *China Synthetic Fiber Industry*, **2007**, *30*,15-18.

[15] Xu DT, Zhu XS, Xu Y, *Polymer Materials Science and Engineering*, **2007**, *23*,
    132-135.

CHAPTER 4: Hydrophilic nonwovens made of cross-linked fully hydrolyzed PVA electrospun nanofibers

Abstract

Fully hydrolyzed poly (vinyl alcohol) (PVA) nanofibers were successfully electrospun from aqueous solutions of PVA in the presence of acetic acid. A continuous spinning of uniform PVA nanofibers proceeded by the addition of acetic acid due to the changes of electronic conductivity and surface tension of aqueous solution of PVA. When cross-linking agent 1 was added to aqueous solution of PVA and subsequent thermal treatment of as-spun nanofibers, chemically cross-linked PVA nanofibers were achieved to resist disintegration in contact with hot water and the tensile mechanical property of nanofiber nonwovens was greatly improved by the formation of cross-linking points. Magnetite was deposited uniformly onto the hydrophilic surface of cross-linked PVA nanofibers and the resulted nanofibers decorated with magnetite showed a magnetic responsiveness. The deposition of magnetite on the PVA nanofibers can generate self-standing magnetic nonwovens.

4.1 Introduction

Nanofibers, which are defined as fibers with diameter less than 1000 nm and the ratio between length and diameter above 1000 times, have been paid special attention due to their promised applications. The nanofibers have a far larger surface area than that of conventional fibers and can exhibit the unique potential functions. Electrospinning is a simple method for producing nanofibers and non-wovens for various applications [1]. It involves discharging a polymer solution in air from a nozzle under high voltage and producing nanofibers by exploiting electrostatic repulsion of the polymer solution. A lot of organic polymers and inorganic precursors have been used as a raw material of electrospun nanofibers and explored their functions originated from their nanofibrous morphology [2]. However, the main drawbacks of these nanofibers are their poor mechanical property and unstability of nanofibrous morphology. To avoid these drawbacks, several attempts have been achieved.

Poly(vinyl alcohol) (PVA) , which is a water-soluble and biocompatible material,

has been widely used in soft contact lenses, drug delivery matrices, cartilage implants, temporary skin covers or burn dressings and artificial organs [3]. While PVA electrospun nanofibers have been prepared by the electrospinning method and investigated their functions [4-10], PVA nanofibers can not maintain their fibrous morphology in water owing to high hydrophilicity of PVA. To improve water resistance and thermal stability needs the enhancement of PVA crystallinity and the formation of cross-linking points. Conventional PVA fibers have been produced from fully hydrolyzed PVA having a higher crystalline degree than partially hydrolyzed PVA [3]. Yao *et al.* found that fully hydrolyzed PVA nanofibers successfully fabricated in the presence of a surfactant to lower the surface tension [11]. Chemical cross-linking of PVA fibers can also improve its stability [3]. Chemical cross-linking is advantageous because it can improve stability of fibrous morphology in all solvents and the mechanical properties. Glutaraldehyde, maleic anhydride, glyoxal, and blocked isocyanate prepolymer have been investigated as chemical cross-linking agents for PVA nanofibers [12-16]. However, these fiber morphologies were changed after immersed in water at room temperature. In this context, the cross-linking process in electrospun PVA nanofibers needs to be explored further.

In this study, we report on the preparation of PVA nanofibers cross-linked with N,N'-trimethylene-bis[2-(vinylsulfony) acetamide] **1**. The cross-linked PVA nanofibers exhibited no morphological change in hot water treatment. The resulted nonwovens provide a specific hydrophilic surface, and the surface can act as a template for the deposition of inorganic materials around the nanofibers.

4.2 Materials and methods

4.2.1 Materials

Two 99.9% hydrolyzed PVA samples (DP=1,700 and 3,200) were provided by Kuraray Co. Ltd, Tokyo, Japan. Partially hydrolyzed PVA2000 (DP=3100, 88 % hydrolyze degree) was purchased from Tokyo Chemical Industry Co. Ltd, Tokyo, Japan. Acetic acid was purchased from Wako, Osaka, Japan. Cross-linking agent **1** was provided from Fujifilm Co. Ltd, Tokyo, Japan. All chemicals were of analytical grade and were used without further purification.
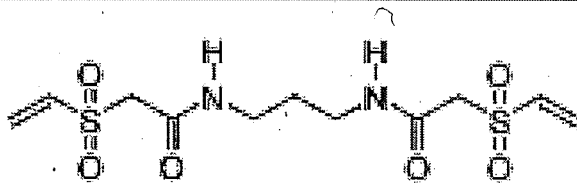
4.2.2 Characterization

The conductivity and surface tension of PVA solutions were measured using a conductivity meter (EC Testr11+, Eutech Intruments Co. Ltd, USA) and a Wilhelmy plate method with a tensiometer (CBVP-Z, Kyowa Interface Science Co. Ltd, Saitama, Japan), respectively. Viscosities were measured using a viscometer (VM-10A, CBC Co. Ltd, Tokyo, Japan) at 25°C. Fiber morphology, average fiber diameter and distribution of the electrospun PVA fibers were characterized using scanning electron microscopy (SEM) (VE-8800, Keyence Co. Ltd, Tokyo, Japan) and field-emission scanning electron microscopy (FE-SEM) (S-5000, Hitachi High-technologies Co. Ltd., Tokyo, Japan). Differential scanning calorimeter (DSC) (DSC 6200, Seiko Instruments Inc. Japan) was used to characterize the thermal properties of the electrospun PVA nonwovens. A piece of non-wovens (2-5 mg) was placed in an aluminum sample pan and heated from 30 to 350 °C at 10 °C/min under N_2. The chemical structure of nanofibers was conducted with a FT-IR (IRPrestige-21, Shimadzu, Japan). Mechanical properties were performed with a tension tester (RTC-1250A, A&D Co., Ltd, Japan) at a constant strain rate of 2mm/min (chuck distance 40mm). Tensile specimens were prepared in size of 40 x 5 mm^2 with a thickness ca. 20 µm and represented average values of at least ten tests. The stability in water of the electrospun nanofibers was estimated by immersing the electrospun nanofiber nonwovens in water at fixed temperature followed by vacuum drying at room temperature for two days. Weight loss was calculated by the weight change before and after immersion test in the dry state and represented average values of ten tests.

4.2.3 Deposition of magnetite layers onto cross-linked PVA nanofibers

$FeCl_3$ $6H_2O$ (5.7 mg, 21.1 µmol) and $FeCl_2$ $4H_2O$ (2.1 mg, 10.5 µmol) were dissolved in 8 ml of distilled water and the aqueous solution was degassed by N_2 [17]. The nanofiber nonwoven (0.5 mg) was immersed within the degassed aqueous

solution of ferrous and ferric ions and stood for 1 hr. After 1 h, 21.2 M NaOH aqueous solution (0.5 ml) was added slowly and the mixture was heated to 90 °C for 40 min. After cooling to room temperature, nonwovens were washed with water and dried under vacuum.

4.3 Results and discussion

4.3.1 Fully hydrolyzed PVA nanofibers

Commercial production of PVA fiber is carried out by wet-spinning using PVA aqueous solution [3]. Since the degree of hydrolysis strongly affects water resistance and mechanical properties of PVA fiber, fully-hydrolyzed PVA is a preferred raw material for fiber formation because of its high crystallinity. In the past decade, the electrospinning of PVA aqueous solution has been intensively investigated, but most of the researches are based on partially hydrolyzed PVA with 88-96 % hydrolysis degree [4-10]. Electrospun nanofibers of partially hydrolyzed PVA with 88 % hydrolysis degree were easy to change their fibrous morphologies in contact with water and showed weak mechanical properties. To improve water resistance and mechanical performance of PVA nanofibers, we selected fully hydrolyzed PVA as a raw material of electrospun PVA nanofibers. The electrospun objects were prepared from 6 w/v% aqueous solutions of partially or fully hydrolyzed PVAs (number average polymerization degree (DP) are 3,100 and 3,200 for partially and fully hydrolyzed PVAs) by applying at 10 kV with a collecting distance of 14 cm. While the partially hydrolyzed PVA can form uniform and long nanofibers with 350 ± 30 nm in average diameter, the aqueous solution of fully hydrolyzed PVA forms only droplets. In addition, no fiber formed from fully hydrolyzed PVA aqueous solutions in the concentration range of 6.0-11.0 wt/v %.
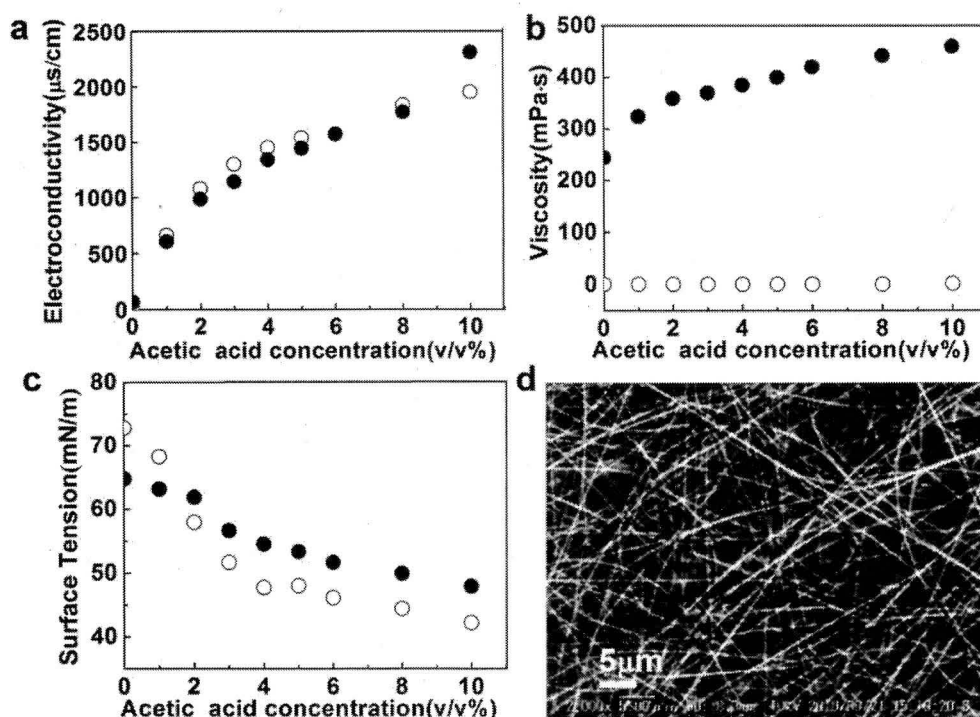
Figure 4.1 Changes in (a) electroconductivity, (b) viscosity, and (c) surface tension of
PVA (DP = 3,200) aqueous solution (●) and water (○) as a function of acetic acid
concentration. (d) SEM images of electrospun fully hydrolyzed PVA nanofibers
prepared from 3.0 v/v% acetic acid aqueous solutions of 6w/v% PVA (DP = 3,200).

In general, continuous and uniform spinning of nanofibers from polymer solutions
through electrospinning process requires adjustments of solution properties such as
surface tension, electroconductivity, and viscosity. Fully hydrolyzed PVA aqueous
solution (6.0 w/v%) revealed a high surface tension at 25°C of 65 mN/m, while
partially hydrolyzed PVA of same concentration showed a much lower value of 39
mN/m. This high surface tension of fully hydrolyzed PVA is one of limiting factors
for the electrospinning process. A low surface tension is favorable for electrospinning
process because of the smooth ejection of the jet from the Taylor cone [1]. Yao et al.
found that aqueous solutions of fully hydrolyzed PVA without any additives did not
form nanofibers due to their high surface tension and successfully accomplished with
the use of Triton X-100 to reduce the surface tension of the PVA aqueous solution
[11]. The addition of additives for the reduction of surface tension is an effective
approach to improve the electrospinning process [18]. However, the additives remain
within the nanofibers and the remained additives may affect final properties of

nanofibers [5-6, 11]. We selected acetic acid as an additive, and acetic acid can evaporate during the electrospinning process [19]. Changes of solution properties of PVA solutions as a function of acetic acid concentration were shown in Figure 4.1(a-c). With the concentration of acetic acid increased from 0 to 3.0 v/v%, the surface tension of the solution declined from 65 to 57 mN/m and the electroconductivity was enhanced from 67 to 1144 μs/cm. Although 4.0 v/v% aqueous ethanol solution (surface tension: 52 mN/m, electroconductivity: 96 μs/cm, viscosity: 191 mPa s) showed a similar surface tension as 3.0 v/v% acetic acid solution, aqueous ethanol solution of fully hydrolyzed PVA formed beaded nanofibers. When 0.1 wt% sodium chloride was employed to adjust a similar electroconductivity (surface tension: 67 mN/m, electroconductivity: 1377 μs/cm, viscosity: 308 mPa s) as that of 3.0 v/v% solution of acetic acid, the electrospinning of this solution formed only droplets without fibers. These results show that adjustment of both surface tension and electronic conductivity are essential for the continuous and uniform spinning of nanofibers from solution of fully hydrolyzed PVA. Acetic acid is a vaporous additive to reduce the surface tension and enhance the electronic conductivity of aqueous solutions.

When acetic acid was added to 6.0 wt/v% solution of fully hydrolyzed PVA, long and smooth nanofibers were formed without beads and the average diameter of PVA nanofibers was 260 ± 25 nm (Figure 4.1d). FT-IR spectrum of nanofibers did not show the characteristic peaks of carboxylic and ester groups (Figure 4.2). This indicates almost completely evaporation of acetic acid during the electrospinning and drying processes (vacuum for 12 h at room temperature). No formation of acetates by the polymer reaction with acetic acid. Furthermore, the melting point of PVA nanofiber measured from DSC curve was found to be 224 °C, which is consistent with that of the powdered sample (220 °C) [13, 20-22]. Addition of acetic acid to aqueous solution of fully hydrolyzed PVA reduced the formation of beads due to the reduction of surface tension, and produced nanofibers with a narrow diameter distribution.
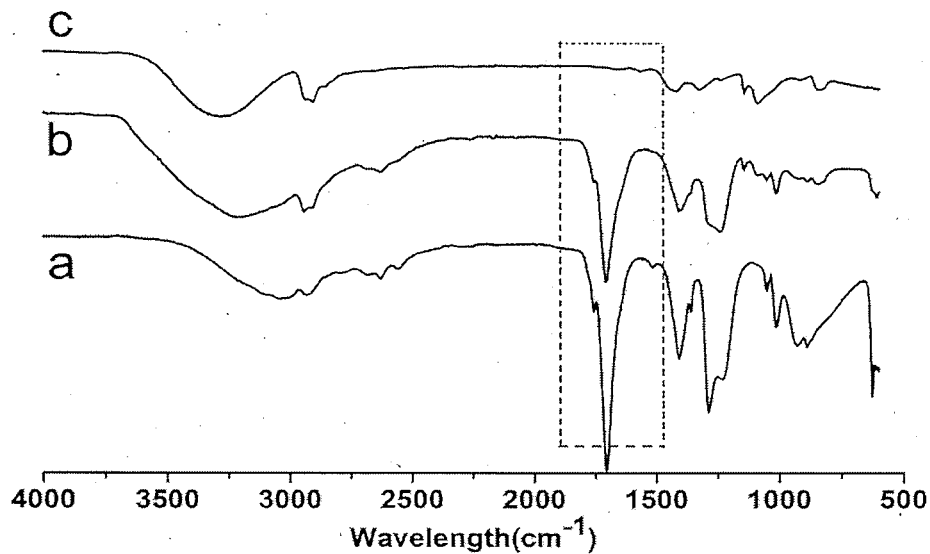
Figure 4.2 FT-IR spectra of (a) acetic acid, (b) as-spun PVA fibers, and (c) PVA
fibers under vacuum for 12 h.

The nanofiber morphologies were investigated by varying the concentration of
acetic acid in 6.0 w/v% solution of fully hydrolyzed PVA (Figure 4.3). When the
concentration of acetic acid was 1.0 wt%, a few beaded fibers were formed but the
majority was droplets. When the concentration increased up to 2.0 wt%, uniform
fibers with an average diameter of 222 ± 46 nm were obtained on the target.
However, there were still some droplets collected on the target, indicating an
unstable electrospinning. PVA solutions containing above 3.0 wt% acetic acid
indicate a steady electrospinning without droplets and uniform nanofibers were
collected onto the target electrode. The average diameter of obtained PVA nanofibers
increased from 260 ± 25 nm to 350 ± 37 nm with the increase of concentration of
acetic acid from 3.0 to 10.0 v/v%.
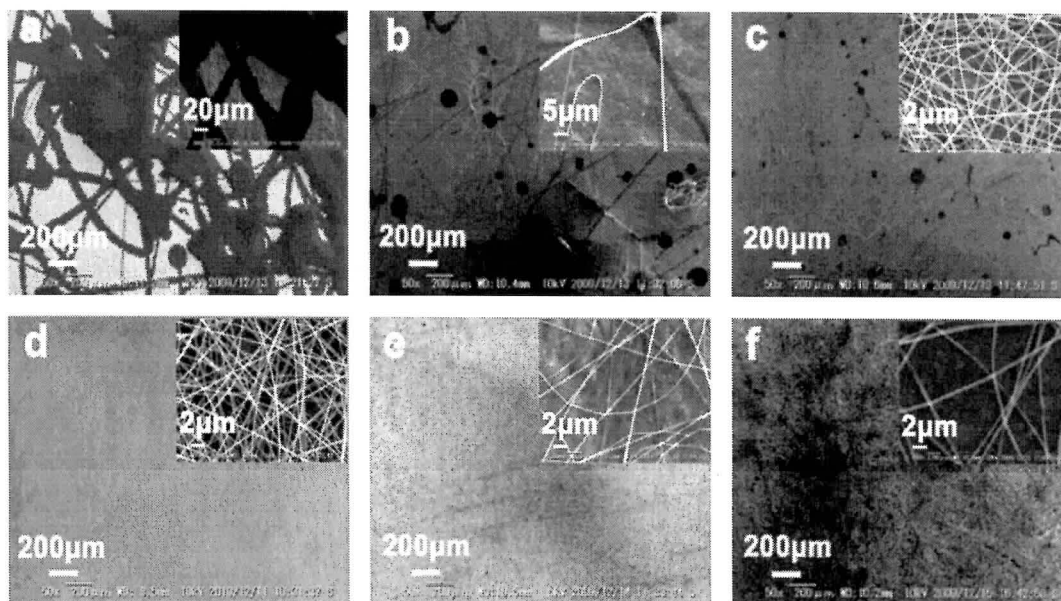
Figure 4.3 SEM images of PVA nanofibers (PVA concentration: 6w/v%) prepared at different acetic acid concentrations; (a) 0wt%, (b) 1wt%, (c) 2wt%, (d) 3wt%, (e) 4wt% and (f) 10wt%.
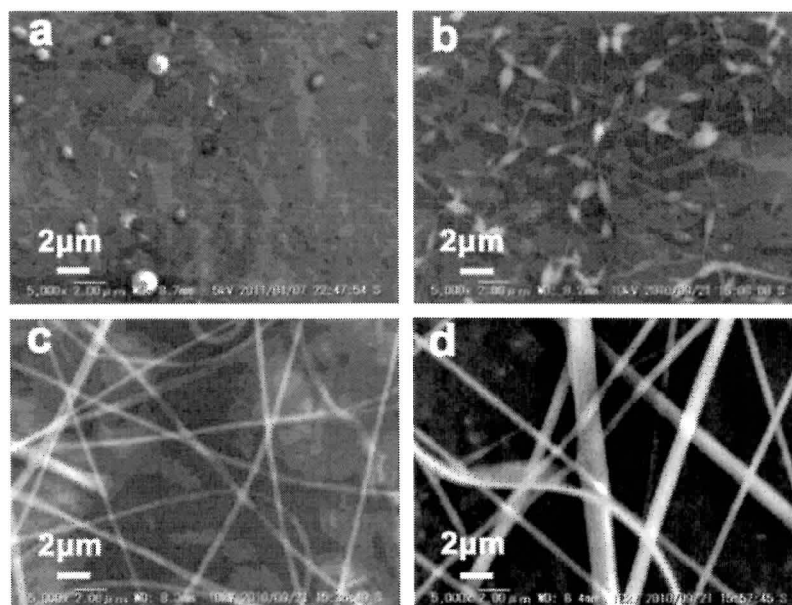
Figure 4.4 SEM images of PVA nanofibers (acetic acid concentration: 3wt%) prepared at different PVA concentrations; (a) 2wt%, (b) 5wt%, (c) 7wt% and (d) 9wt%.

The effect of concentration of fully hydrolyzed PVA on the morphology of electrospun nanofibers was investigated by varying the PVA concentrations containing 3.0 wt% acetic acid (Figures 4.4 and 4.5). Only beads were collected on

the target from 2.0 w/v% aqueous solution of fully hydrolyzed PVA. When the PVA conceuntration was increased to 3.0 w/v%, beaded fibers were found on the target. Completely beads-free fibers with an average diameter of 260 ± 25 nm were formed at 6.0 w/v%. The nanofibers prepared from 9.0 w/v% PVA solution became much wider with an average diameter of 766 ± 155 nm.
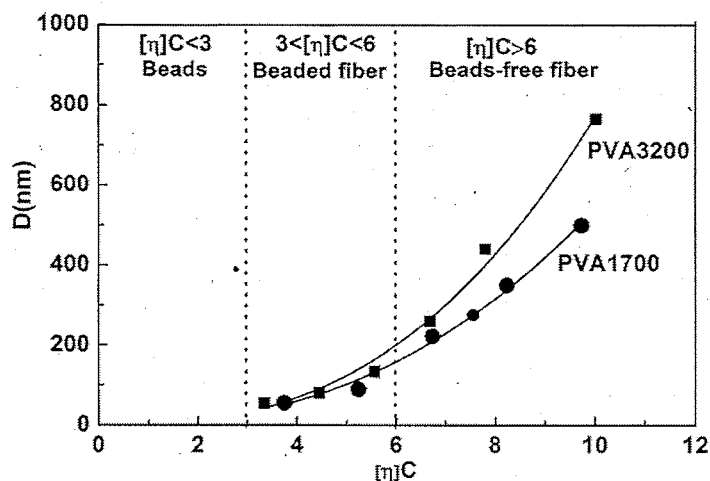
Figure 4.5 Diameter dependence on PVA concentrations.

When the nonwovens composed of electrospun PVA nanofibers were immersed into water, the nonwoven instantaneously shrank and turned into globular gels. Fibrous structures were lost by the immersion of nonwovens into water. The weight losses of nanofiber nonwovens after immersing into water at 37 °C for 2 hr were · measured. The nanofiber nonwoven made of partially hydrolyzed PVA completely dissolved in water. In contrast, the nonwovens made of fully hydrolyzed PVA showed a 26 % of weight loss, indicating a better water-resisting property than partially hydrolyzed PVA. The degrees of crystallinity of nanofibers determined by the DSC analyses were found to be 17 and 35 % for partially and fully hydrolyzed PVAs, respectively. The presence of acetate groups in PVAs diminishes the formation of hydrogen bonding among polymer chains and reduces the degree of crystallinity. · The use of fully hydrolyzed PVAs has a great advantage to improve water resistance · of nanofiber nonwovens. Furthermore, the mechanical properties of nonwovens made of fully hydrolyzed PVAs revealed higher tensile strength and strain values compared to that of partially hydrolyzed PVA. This suggests that the high degree of crystallinity enhanced the mechanical properties of nanofiber nonwovens.

Table 4.1 Physcial properties and water resistance of PVA nanofibers

DP of PVA	1,700[a]	3,200[a]	3100[b]
Melting point (°C)	216	221	191
Degree of crystallinity (%)	29	35	15
Tensile strength (MPa)	6.1 ± 3.1	12.0 ± 2.3	5.3±1.9
Enlongation at break (%)	56.7 ± 6.8	114.2± 14.5	32.7±5.8
Weight loss in water[c] (%)	26 (0[d])	17 (0[d])	100 (35[d])

[a] Fully hydrolyzed PVA, [b] Partially hydrolyzed PVA, [c] 37°C for 2 hr, [d] after thermal treatment at 180°C for 10 min

Nanofiber formations of two fully hydrolyzed PVAs having DP = 1,700 and 3,200 were investigated. Uniform nanofibers were obtained from aqueous PVA solutions containing acetic acid. Low molecular weight PVA (DP=1,700) formed beads-free nanofibers from the PVA solutions containing 3.0 v/v% acetic acid in the PVA concentration ranges of 9.0-13.0 wt/v%. PVA nanofibers with two different molecular weights showed different properties (Table 4.1). Fully hydrolyzed PVA nanofibers revealed an increase in melting point from 216 to 221 °C and in degree of crystallinity from 29 to 35 % as increasing of molecular weight from 1,700 to 3,200. The tensile strength of nanofiber nonwovens also enhanced according to the increase of molecular weights.

4.3.2 Thermal Treatment
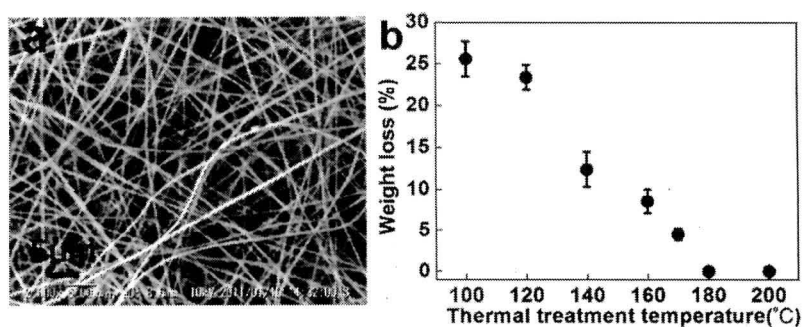
Figure 4.6 a) SEM image of thermal treated PVA (DP = 3,200) nanofibers after immersing water at 37 °C for 2 h (b) Weight losses of PVA (DP = 3,200) nanofibers treated at different temperatures after immersing water at 37 °C for 2 h.

Although the nanofiber nonwovens made of fully hydrolyzed PVA (DP = 3,200) exhibited better water resisting property compared to partially hydrolyzed PVA, the morphology of nanofibers was lost by the immersing into water, suggesting that water resistance of as-spun nanofiber nonwovens is not enough. For the conventional PVA fibers produced by wet-spinning, post-thermal treatment has been employed to improve their water resisting property [3]. The nanofiber nonwoven treated at 180 °C for 10 min showed no weight loss by the immersing in water at 37 °C for 2 hr, indicating the improvement of water resistance of PVA nanofiber nonwovens by the post-thermal treatment. The heat-treated nanofibers maintained a fibrous morphology and the average diameter of immersed nanofibers was enlarged from 260 ± 25 nm to 420 ± 30 nm (Figure 4.6a). In contrast, the partially hydrolyzed PVA nanofibers did not show the enhancement of water resistance by the heat treatment at 180 °C. The weight loss of fully hydrolyzed PVA nanofibers was gradually decreased as increasing temperature of thermal treatments (Figure 4.6b). The nanofibers treated below 180 °C changed no-structural materials by the immersing in water.

4.3.3 Cross-linking

The morphologies of thermal-treated nanofibers by the immersing in water kept below 45 °C, but the fibrous structure was completely lost above 50 °C. The thermal treated nanofibers could not maintain their fibrous structures in hot water. For the biomedical applications, the sterilization process of materials is essential to eliminate all forms of microbial life. To achieve the complete water resistance in hot water and steam for the sterilization processes needs the cross-linking among PVA chains within the nanofibers. There are several attempts for the cross-linking of PVA by using several cross-linking agents in the presence of strong acids. Cross-linked PVA nanofibers have been prepared by two methods. One approach is the soaking of electrospun PVA nanofibers with solutions of cross-linking agents in the presence of strong acids or the exposure of nanofibers with vapors of cross-linking agents. Recently, Khan and coworkers succeeded to obtain cross-linked PVA nanofibers through single step electrospinning from PVA aqueous solution containing glutaraldehyde and HCl [16]. *In situ* cross-linking processes can use a conventional setup with no modifications, however, the presence of cross-linking agents and catalytic acids influenced the solution properties of PVA solutions. Thus, the careful

adjustment of solution properties is needed to obtain the cross-linked PVA nanofibers. And there is no report for the complete water resistance in hot water. Compound **1** was used as a water-soluble cross-linking agent for electrospun PVA nanofibers. This cross-linking agent has been used for the preparation of water-insoluble materials by the formation of cross-linking points among water-soluble polymers including gelatins and starches. The vinylsulfonyl groups in **1** react with hydroxy groups in PVA without the use of catalytic acid. The aqueous mixture of PVA and **1** at room temperature do not cause gelation by the formation of cross-linking points and keep stable solution having the same viscosity during several days. This indicates that the cross-linking reaction does not occur in aqueous solution. On the other hand, the dried PVA films prepared from aqueous solution of PVA and **1** exhibits insoluble in water after the thermal treatment at 150 °C. Compound **1** is suitable as a cross-linking agent to obtain *in situ* cross-linked PVA nanofibers though the electrospinning process.
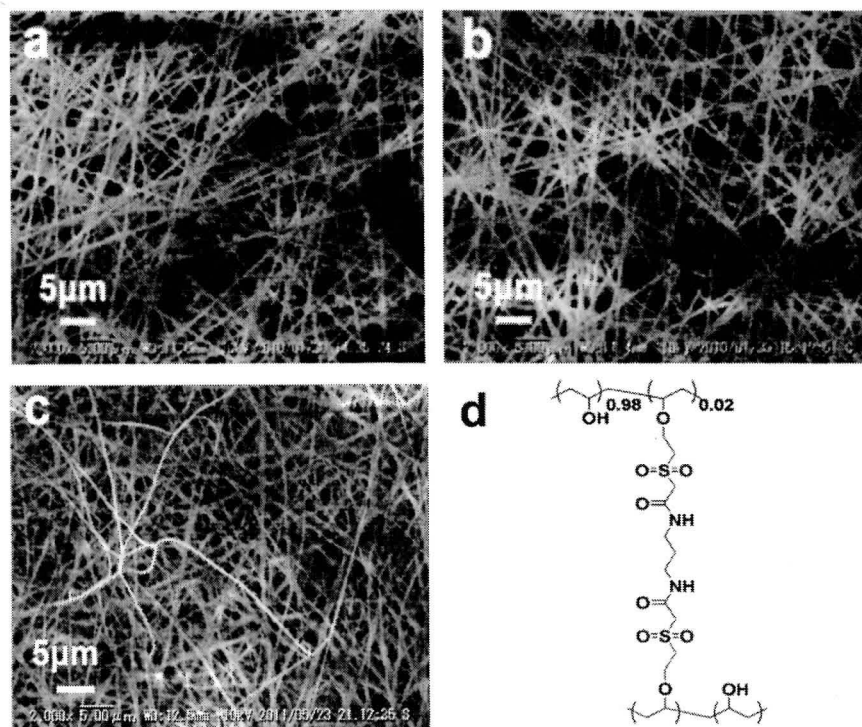
Figure 4.7 SEM images of electrospun PVA (DP = 3,200) nanofibers containing 15.0 wt% **1**; (a) as-spun nanofibers, (b) nanofibers after thermal treatment at 150 °C for 10 min, and (c) nanofibers after immersing in hot water at 90 °C for 2 hr. (d) Proposed chemical structure of cross-linked PVAs.

In order to improve the water resisting property, chemical cross-linking reagent **1** was applied in electrospinning process of fully hydrolyzed PVAs. The nanofiber nonwovens prepared from the mixed solution of fully hydrolyzed PVA (DP = 3,200) and **1** displayed complete resistance to hot water and did not show the change of diameter after the immersing in hot water. (Figure 4.7a) Uniform nanofibers were obtained from the electrospinning of mixed aqueous solution of PVA with **1** and 3.0 v/v% acetic acid, and the average diameter of nanofibers containing **1** was almost the same as nanofibers prepared from PVA aqueous solution without **1**. The concentration of **1** was 15.0 wt%, which is equal to 2 mol% against the number of hydroxy groups in PVA. This suggests that the presence of **1** did not affect the solution properties of PVA aqueous solution (surface tension: 57 mN/m, electroconductivity: 1214 μs/cm, viscosity: 352 mPa s). After heating at 150°C for 10 min, no changes of fibrous structure were observed as shown in Figure 4.7b. After immersion in hot water for 2 h, the cross-linked PVA nanofibers showed only a weight loss of 0.4%, the morphology and the average diameter of nanofibers remained no altered, revealing the complete resistance in hot water at 90 °C.
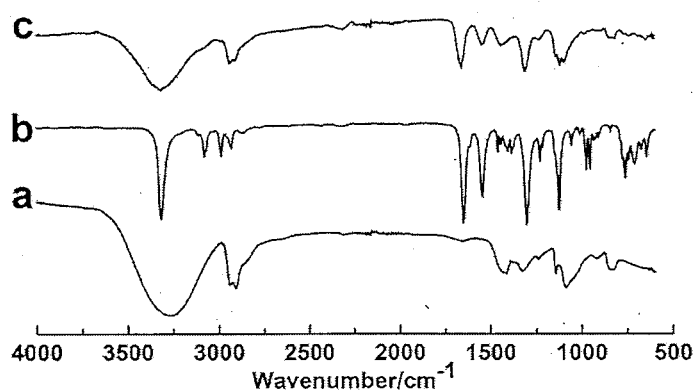
Figure 4.8 FT-IR spectra of (a) PVA, (b) **1**, and (c) cross-linked PVA nanofibers.

The formation of cross-linking points in PVA nanofibers can be monitored by FT-IR spectrum and DSC. As shown in Figure 4.8, the FT-IR spectrum of cross-linked nanofibers showed the peak at 1660 cm^{-1} attributed to the -C=O stretching vibration of **1** as well as a broad characteristic peak at 3300cm^{-1} attributed to the -OH stretching vibration of PVA[3, 5]. Furthermore, compared to the spectrum

of as-spun nanofibers before heating, the peaks at 3082 and 975 cm^{-1} attributed to the vibration of vinyl segments almost disappeared, which indicated the chemical reaction between hydroxyl group of PVA and double bond of **1**. Cross-linked PVA nanofibers showed lower melting point (180 °C) and degree of crystallization (24%) than PVA nanofiber lacking cross-linking points (Table 4.1). The induction of cross-linking points would decrease the regularity of PVA molecular chain and suppress the crystallization of PVA. Therefore, the incorporated cross-linking agent **1** within PVA nanofibers reacted with hydroxyl side chains in PVA and formed the cross-linking points within the polymer matrix.
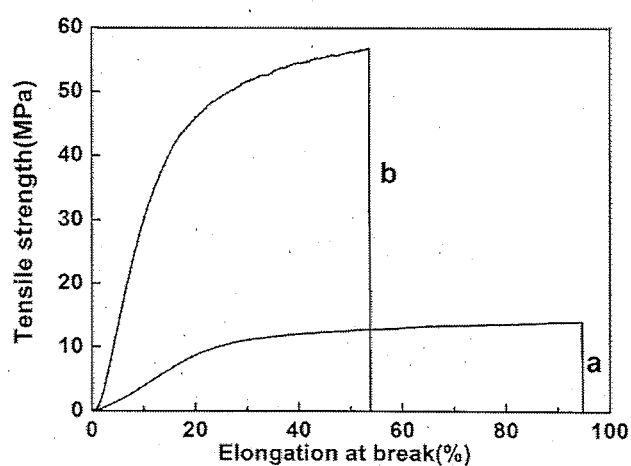
Figure 4.9 Tensile profiles of (a) as-spun and (b) cross-linked PVA nanofibers.

The cross-linking in the polymer matrix would enhance the tensile mechanical strength of PVA nanofibers. Lee *et al.* successfully enhanced the tensile strength of partially hydrolyzed PVA nanofiber nonwovens by seven times in presence of a blocked isocyanate prepolymer as a cross-linker [15]. The tensile mechanical performance of cross-linked PVA nanofibers was significantly improved compared with that of the pristine PVA nanofibers (Figure 4.9). The tensile stress increased from 14.0 ± 1.8 to 56.8 ± 4.6 MPa and the elongation at break of the nanofibers decreased from 94.6 ± 10.2 to 53.6 ± 8.2% by the formation of cross-linking points.

4.3.4 Deposition of magnetite layer on PVA nanofiber
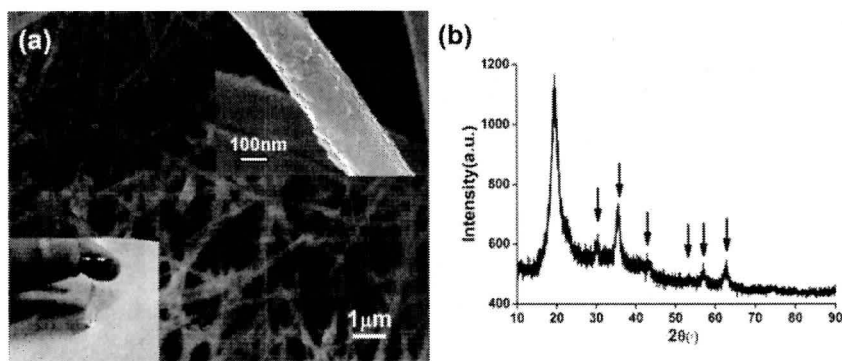
Figure 4.10 (a) SEM images of PVA nanofibers deposited with magnetite layer. The insets show FE-SEM image and the magnetic responsiveness of nanofiber mat to the applied magnet and (b) XRD pattern of PVA nonwoven deposited with magnetite layer.

Recently, water-soluble polymers including PVA have been used as capping regents to stabilize various metal nanoparticles [23-27]. Within the metal nanoparticles, magnetite nanoparticles with a controlled size have attracted increasing interests due to their superparamagnetism and low toxicity for bio-medical applications [28-31]. To date, several groups reported on magnetic nanofibers by mixing pre-prepared magnetite nanoparticles or precursors with polymer solution and followed by the electrospinning process [32, 33]. In contrast, we prepared magnetic nanofibers by a simple way using the hydrophilic surface of the PVA nanofibers. We prepared the magnetic non-wovens by the deposition of magnetite on the cross-linked PVA nanofibers according to the modified method for the preparation of magnetite nanoparticles [17]. During the deposition process of magnetite, the color of nonwoven was changed from white to pale-brown. The SEM image revealed a uniform deposition of magnetite layer onto the surface of PVA nanofibers and no formation of large magnetite particles (Figure 4.10a). The average diameter of magnetite-deposited nanofibers is 295 ± 40 nm (the average diameter of parent PVA nanofiber is 250 ± 27 nm) and the thickness of magnetite layer around PVA nanofibers is about 25 nm. The preservation of fibrous morphology also indicated the high-stability of cross-linked PVA nanofibers. The XRD pattern of nonwoven deposited with magnetite layer showed five diffraction peaks at $2\theta = 30.2$, 35.6, 43.3, 53.5, and 57.2° (Figure 4.10b). These peak positions agree with (220),

(311), (400), (422) and (511) crystallographic planes of the spinel phase Fe_3O_4 [34, 35]. The uniform deposition of magnetite layer is mainly attributed to the complexation of iron ions or magnetite nanoparticles with the hydroxy groups in PVA. The treated nonwoven exhibited a magnetic responsiveness to the applied magnet as shown in the inset of Figure 4.10. Investigations are underway to evaluate magnetic properties by vibrating sample magnetometer. The hydrophilic PVA nanofibers worked as a template for the formation of magnetic nanofibers by the deposition of magnetite layer.

4.4 Conclusion

Fully hydrolyzed PVA nanofibers were successfully prepared by the electrospinning method using PVA aqueous solutions in the presence of acetic acid. Acetic acid is a vaporous additive to reduce the surface tension and enhance the electronic conductivity of PVA aqueous solution. The adjustment of solution properties of PVA aqueous solutions resulted in the continuous spinning of uniform nanofibers. The concentration of acetic acid and the molecular weight of PVA strongly affected the resulted morphology of PVA nanofibers. The post-thermal treatment of PVA nanofibers and the *in-situ* cross-linking greatly enhanced the water resistance of nanofibers. Especially, the morphology of cross-linked PVA nanofibers did not change after immersing into hot water. Furthermore, the tensile mechanical properties of PVA nanofiber nonwovens were significantly enhanced via cross-linking. We demonstrated the decoration of magnetite nanoparticles onto the surface of the cross-linked nanofibers. The nanofibers with magnetite showed the same morphology as the parent nanofibers and revealed a magnetic property. The cross-linked PVA nanofibers can open new possibility for the creation of functional nanocomposite materials by combining various nanomaterials.

References

[1] Greiner A, Wendorff JH. *Angew. Chem. Int. Ed.*, **2007**, *46*, 5670-5703.

[2] Nguyen LTH., Chen S., Elumalai NK, Prabhakaran, MP, Zong Y, Vijila C, Allakhverdiev, SI and Ramakrishna, S. *Macromol. Mater. Eng.*, **2012**, doi: 10.1002/mame.201200143.

[3] Sakurada I. Polyvinyl alcohol fibers, ed. by Lewin M. Marcel Dekker Publishers,

New York, **1987**, pp 62-67.

[4] Theron SA, Zussman E, Yarin AL. *Polymer*, **2004**, *45*, 2017-2030.

[5] Koski A, Yim K, Shivkumar S. *Mater. Lett.*, **2004**, *58*, 493-497.

[6] Lee JS, Choi KH, Ghim HD, Kim SS, Chun DH, Kim HY, Lyoo WS. *J. Appl. Polym. Sci.*, **2004**, *93*, 1638-1646.

[7] Son WK, Youk JH, Lee TS, Park WH, *Mater. Lett.*, **2005**, *59*, 1571-1575.

[8] Zhang C, Yuan X, Wu L, Han Y, Sheng J, *Eur. Poly. J.*, **2005**, *41*, 423-432.

[9] Yano T, Higaki Y, Tao D, Murakami D, Kobayashi M, Ohta N, Koike J, Horigome M, Masunaga H, Ogawa H, Ikemoto Y, Moriwaki T, Takahara A. *Polymer*, **2012**, *53*, 4702-4708.

[10] Na H, Chen P, Wong SC, Hague S, Q Li. *Polymer*, **2012**, *53*, 2736-2743.

[11] Yao L, Haas TW, Guiseppi-Elie A, Bowlin GL, Simpson DG, Wnek GE. *Chem. Mater.*, **2003**, *15*, 1860-1864.

[12] Ding B, Kim HY, Lee DR, Choi KJ. *Fibers Polym.*, **2002**, *3*, 73-79.

[13] Yang E, Qin X, Wang S. *Mater. Lett.*, **2008**, *62*, 3555-3557.

[14] Taepaiboon P, Rungsardthong U, Supaphol P. *Nanotechnology*, **2007**, *18*, 175102.

[15] Lee JH, Lee US, Jeong KU, Seo YA, Park SJ, Kim HY. *Polym. Int.*, **2010**, *59*, 1683-1689.

[16] Tang C, Saquing CD, Harding JR, Khan SA. *Macromolecules*, **2010**, *43*, 630-637.

[17] Yang D, Hu J, Fu S. *J. Phys. Chem. C*, **2009**, *113*, 7646-7651.

[18] Fong H, Chun I, Reneker DH. *Polymer*, **1999**, *40*, 4585-4592.

[19] Supaphol P, Mit-uppathan C, Nithitanakul M, *Macromol. Mater. Eng.*, **2005**, *290*, 933-942.

[20] Nishio Y, Haratani T, Takahashi T. *Macromolecules*, **1989**, *22*, 2547-2549.

[21] Jiang J, Lee DK, *Polymer*, **2003**, *44*, 8139-8146.

[22] Huang H, Hu Y, Zhang J, Sato H, Zhang H, Noda I, Ozaki Y. *J. Phys. Chem. B*, **2005**, *109*, 19175-19183.

[23] Godovsky DY, *Adv. Polym. Sci.* **2000**, *153*, 163-205.

[24] Kumar RV, Koltypin Y, Cohen YS, Aurbach D, Palchik O, Felner I, Gedanken A. *J. Mater. Chem.*, **2000**, *10*, 1125-1129.

[25] Strawhecker KE, Manias E. *Chem. Mater.* **2000**, *12*, 2943-2949.

[26] Kumar RV, Elgamiel R, Diamant Y, Gedanken A, Norwig J. *Langmuir*, **2001**, *17*, 1406-1410.

[27] Yu YH, Lin CY, Yeh, JM, Lin WH. *Polymer*, **2003**, *44*, 3553-3560.

[28] Häfeli U, Pauer GJ, Teller J, Zborowski M. Scientific and clinical applications of magnetic carriers, Plenum Press: New York; **1997**.

[29] Yuan JJ, Armes SP, Takabayashi Y, Prasside K, Leite CAP, Galembeck F, Lewis AL. *Langmuir*, **2006**, *22*, 10989-10993.

[30] Mbhere AH, Salemane MG, van Sittert CGC, Nedeljković JM, Djoković V, Luyt AS. *Chem. Mater.*, **2003**, *15*, 5019-5024.

[31] Mahmoudi M, Simchi A, Imani M. *J. Phys. Chem. C*, **2009**, *113*, 9573-9580.

[32] Santala E, Kemell M, Leskelä M, Ritala M. *Nanotechnology*, **2009**, *20*, 035602.

[33] Wang S, Wang C, Zhang B, Sun Z, Li Z, Jiang X, Bai X. *Mater. Lett.*, **2010**, *64*, 9-11.

[34] Pimpha N, Chaleawlert-umpon S, Sunintaboon P. *Polymer*, **2012**, *53*, 2015-2022.

[35] Si S, Li C, Wang X, Yu D, Peng Q, Li Y. Cryst. *Growth. Des.*, 2005, *2*, 391-393.

CHAPTER 5: Flexible tactile sensor using reversible deformation of poly(3-hexylthiophene) nanofiber assemblies

Abstract

In this paper, we report a simple approach to fabricating scalable flexible tactile sensors using a nanofiber assembly of regioregular poly(3-hexylthiophene) (P3HT). Uniform P3HT nanofibers are obtained through a continuous electrospinning process using a homogeneous solution of high-molecular-weight P3HT. The P3HT nanofibers are oriented by collecting them on a rotating drum collector. Small physical inputs into the self-standing P3HT nanofiber assemblies give rise to additional contact among neighboring nanofibers, which results in decreased contact resistance in directions orthogonal to the nanofiber orientation. The P3HT nanofiber assemblies could detect pressure changes and bending angles by monitoring the resistance changes, and the sensor responses were repeatable.

5.1 Introduction

Biological and artificial materials contain hierarchical structures composed of structural elements possessing different size scales, and the structural hierarchy plays an important role in determining the bulk properties [1]. The construction of hierarchical structures based on nano- and microstructures can give rise to improved or more useful physical properties. Recently, several groups have demonstrated flexible skin-like electronic sensors through the creation of ordered structures on flexible substrates [2-4]. These sensors can detect pressure, strain, and bending changes through the deformation of nano- or microstructures. Assemblies of 1D fibrous structures have also been used as sensing units in the skinlike electronic sensors[5, 6]. A flexible carbon nanotube (CNT) strain sensor has been demonstrated by Hata et al. in which CNT thin films aligned on flexible substrates could sense strains in response to the expansion of a CNT film [7]. Suh et al. developed a strain-gauge sensor based on nanoscale mechanical interlocking between two arrays of metal-coated nanofibers [8]. The assembly of tiny fibers is a useful microstructure for monitoring minute pressure changes.

Regioregular poly(3-alkylthiophene)s (P3HTs) are the most prominent organic semiconductors applied in organic electronics involving organic field-effect transistors and solar cells [9, 10]. Nanoscale P3HT fibers have been fabricated using various techniques, such as self-organization in solutions [11,12] and electrospinning [13], and their electronic properties have been investigated. Electrospinning is a simple method for producing long and continuous fine fibers with diameters ranging from 10 nm to submicrometers [14]. Because of the absence of chain entanglement of rigid rodlike P3HT in a solution, the continuous spinning of uniform P3HT nanofibers requires either mixing with high-molecular-weight insulating polymers or the use of highly concentrated solutions [15-20]. The mixing of conductive P3HT with nonconductive polymers has resulted in a lower conductivity compared to that of pure P3HT. To avoid this drawback, core-shell nanofibers embedding P3HT nanofibers have been fabricated by coaxial electrospinning using sacrificial shells [21-25]. To obtain the pure P3HT nanofibers, the shell layers needed to be removed from the core-shell nanofibers, and the residual shell layers around the P3HT nanofibers affected the electronic properties. Very recently, Kotaki et al. fabricated pure P3HT nanofibers by electrospinning from a highly concentrated P3HT solution [26]. They found that the physical entanglement among P3HT backbones in highly concentrated solutions improved the spinnability. However, the resulting P3HT nanofibers possessed nonuniform surface structures and scalable nanofiber fabrication was impossible because of the instability of the jet initiation process. To overcome these limitations of pure P3HT nanofiber fabrication, we used a high-molecular-weight regioregular P3HT. The molecular weight of this P3HT is about 10 times higher than that of the P3HT used in previous studies. Our expectation was that the longer length of the rigid P3HT backbone would increase the solution viscosity of a low-concentration solution. This change in solution properties may improve the electrospinning stability in the fabrication of pure P3HT nanofibers. We also expected an enhancement of the mechanical and electronic properties for high-molecular-weight P3HT nanofibers, which is important in terms of developing flexible tactile sensors based on P3HT nanofiber assemblies.

In the present study, we developed a flexible tactile sensor consisting of aligned P3HT nanofiber assemblies. Continuous electrospinning of high-molecular-weight P3HT formed self-standing nanofiber assemblies, and the iodine-doped nanofiber

assemblies exhibited an anisotropic electronic conductivity along with the fiber axis. The interconnecting of nanofibers within the aligned assemblies caused resistance changes in response to pressure changes and bending motions.

5.2 Experimental

5.2.1 Preparation of P3HT nanofibers

P3HT solutions were prepared by dissolving P3HT in chloroform at 58°C with stirring for 4 h. The electrospinning equipment (NANON-01A, MECC, Japan) consists of a syringe with a hollow blunt metal needle spinneret (0.7 mm inner diameter, NN-2238N, Terumo, Japan), a syringe pump for controlled the feed rate, a grounded cylindrical stainless steel mandrel, and a high voltage DC power supply. In a typical electrospinning experiment, P3HT solution was transferred into the syringe and delivered to the tip of the syringe needle by the syringe pump at a constant feed rate (3.0 mL/h). A 12 kV positive voltage was applied to the P3HT solution via the stainless steel syringe needle. The subsequently ejected polymer fiber was collected on the drum collector rotating at 3000 rev/min. The distance between the tip of the needle and the surface of the collector was about 14 cm.

Doping with I_2 was carried out by exposing the P3HT nanofibers into I_2 fume (20g of Iodine in 500 ml bottle) for about 40 min at 25 °C prior to measurement.

5.2.2 Characterization

Fiber morphology, average fiber diameter and diameter distribution of the electrospun P3HT fibers were characterized using scanning electron microscopy (SEM) (VE-8800, Keyence Co. Ltd, Tokyo, Japan). Differential scanning calorimetry (DSC) (DSC 6200, Seiko Instruments Inc. Japan) was used to characterize the thermal properties of the electrospun P3HT mats. A piece of P3HT mat (2-5 mg) was placed in an aluminum sample pan and heated from 50 to 300°C at 10°C/min under a N_2 atmosphere. The crystalline structure of the samples was analyzed using wide-angle X-ray diffraction (XRD; Rotorflex RU200B; Rigaku, Japan). XRD was performed using Ni-filtered Cu Kα radiation ($\lambda = 1.5402$ Å) in a step-scan mode at a rate of 1°/min in the 2θ range 0°–30°. Mechanical properties were performed with a tension tester (RTC-1250A, A&D Co., Ltd, Japan) at a constant strain rate of 2 mm/min (chuck distance 40mm). Tensile specimens of P3HT nanofiber assemblies

were prepared in size of 40 x 5 mm^2 with a 15 μm thickness and represented average values of at least ten tests.

5.2.3 Electrical conductivity measurements

To measure the electrical conductivity of isolated electrospun fibers, twenty aligned fibers were deposited across a pair of gold electrodes (2.0 cm in length and gap width of 1.0 mm) on a glass substrate. The average electrical conductivity (σ), which is the inverse of the electrical resistivity, can be calculated by the following equation,

$$\sigma = 4\gamma \, / \, n\pi d^2 R$$

where R is the resistance measured on the parallel Au electrodes, n is the number of parallel pathways formed by fibers bridging over the contiguous electrodes as measured by digital optical microscopy (KH-7700, Hirox, Japan), d is the average fiber diameter obtained by scanning electron microscopy (VE-8800, Keyence Co. Ltd, Tokyo, Japan), and γ is the interelectrode distance of Au. Assuming that the fiber segments act as resistances in parallel, the single-fiber resistance is $R_f = nR$.

5.2.4 Pressure sensing test

Pressure sensing test was performed on a P3HT assembly with a square of 2.0 cm. Ag paste is applied as the electrodes connected the P3HT assembly to the measurement system. The resistance changes were monitored by using a source meter (2612 System Source meter, Keithley, USA) in response to mechanical loads.

5.3 Results and discussions

The P3HT nanofiber assemblies were fabricated by the conventional electrospinning process from a homogeneous CHCl$_3$ solution of high-molecular-weight P3HT (Soken Chemical & Enginnering; Verazol HT-030; M_w = 300-500 K g/mol, M_w/M_n = 2.0-3.5, Regioregularity > 99%). When low-molecular-weight P3HT (Aldrich; electronic grade, M_n = 54-75K g/mol, M_w/M_n < 2.5, Regioregularity > 98%) was dissolved in CHCl$_3$ at 60 °C and then cooled to room temperature, the color of the solution changed from orange to dark brown, indicating the formation of interpolymer aggregates through strong π-π interaction among rigid P3HT backbones. Shimomura et al. reported that the P3HT in solvents self-organized into nanofibers through interpolymer interactions [27]. The formation of self-organized nanofibers in the solution resulted in an unstable electrospinning

process. In contrast, the color of the high-molecular-weight P3HT solution remained unaltered after cooling to room temperature. Moreover, the viscosity of this solution at 4.0 w/v % was maintained over 12 hrs. The P3HT solution at 4.0 w/v% showed a continuous spinning until the end of solution supply at room temperature (8 h at a 3.0 mL/h feed rate), and bead-free uniform nanofibers were collected as nanofiber mats on the target electrode.
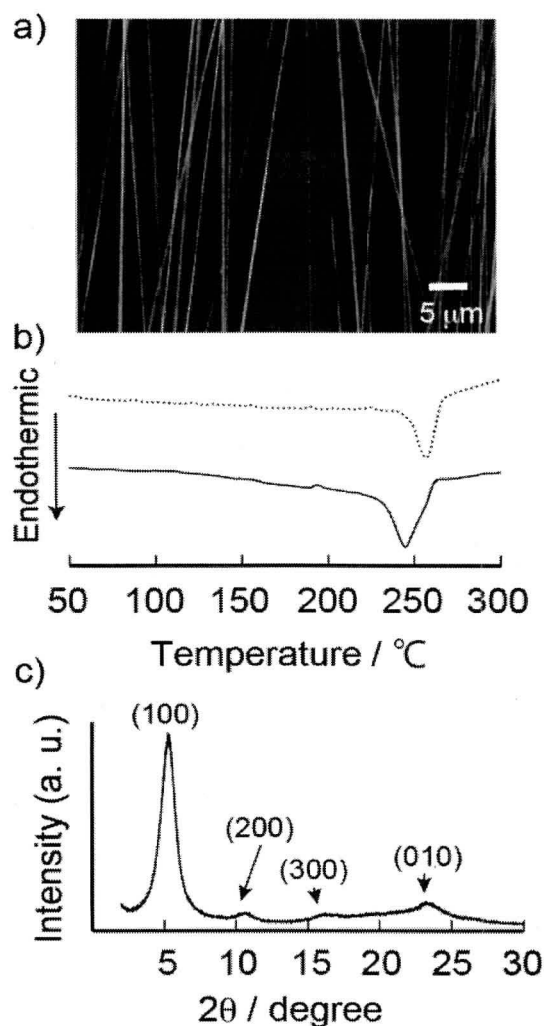
Figure 5.1 (a) SEM image of aligned electrospun P3HT nanofibers. (b) DSC diagrams for the first heating of P3HT nanofibers (solid line) and powdered P3HT (dotted line). (c) XRD pattern of P3HT nanofibers.

Figure 5.1a shows the SEM images of aligned P3HT nanofiber assemblies as prepared by electrospinning using a rotating drum collector at a fiber take-up velocity of 940 m/min. The resulting P3HT nanofibers displayed ribbonlike morphology with an average width of 811 ± 115 nm and an average thickness of 61 ±

10 nm. Although substantial misalignment was still observed in the fiber assemblies, the orientation parameter of the nanofiber assemblies estimated by statistical analysis of the direction histogram was found to be 89 %, suggesting that the nanofibers were oriented within ± 20° of the preferred direction. A differential scanning calorimetry (DSC) profile of the P3HT nanofiber showed one endothermic peak at 246 °C, which was attributed to the melting point (Figure 5.1b) [28]. The observed melting point was slightly lower than that of the powdered sample ($T_m = 257$ °C), and the peak was broader. These differences in DSC seem to indicate the suppression of large crystalline domain formation within the P3HT nanofibers. An X-ray diffraction (XRD) pattern of P3HT nanofibers displayed three diffraction peaks indexed as (100), (200), and (300) (Figure 5.1c) [28]. The positions of the diffraction peaks almost agree with those of the P3HT thin film, indicating the presence of a crystalline lamellar structure in the P3HT nanofibers. Moreover, a (010) diffraction peak due to the π-π stacking among poly(thiophene) backbones was observed. The dissolved high-molecular-weight P3HT crystallized during the electrospinning process, and the nanofibers then embedded the P3HT microcrystallines.
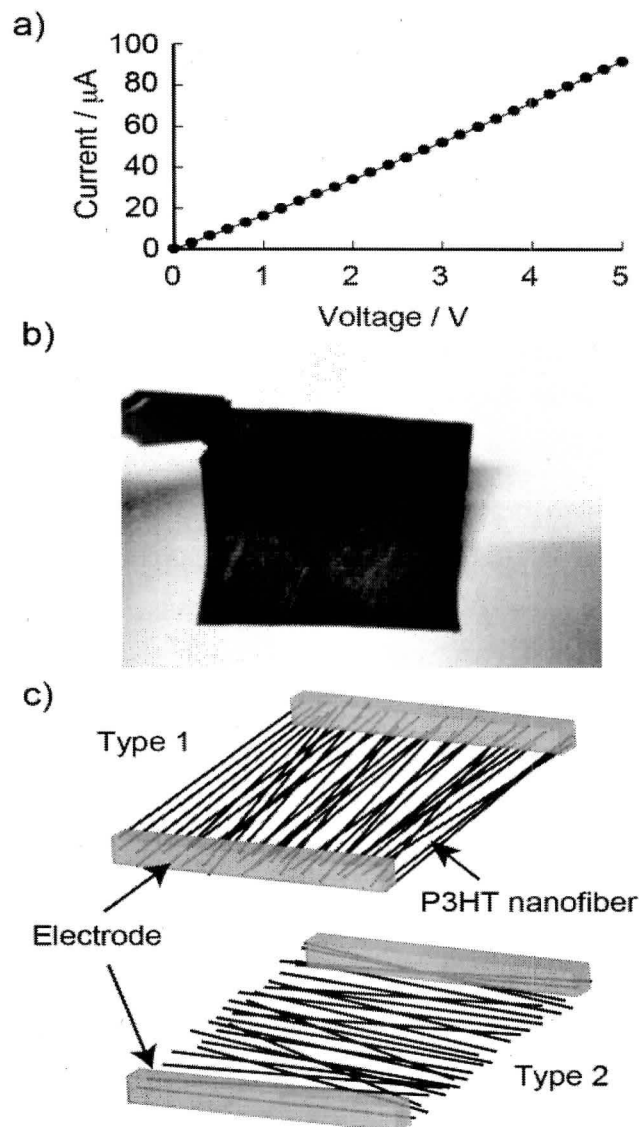
Figure 5-2. (a) *I-V* curves of twenty P3HT nanofibers after I_2 doping. (b) Photograph of aligned P3HT nanofiber assembly (2 x 2 cm). (c) Schematic of two arrangements of electrodes (types 1 and 2) on P3HT nanofiber assembly.

Figure 5-2a shows the current-voltage (*I-V*) characteristics of the P3HT nanofibers at room temperature. Twenty P3HT nanofibers were deposited across a pair of gold electrodes (2.0 cm in length with a gap width of 1.0 mm) on a glass substrate, and the fibers did not contact with each other (as confirmed by optical microscopy). The current increased exponentially with increasing voltage, which is a typical semiconductive characteristic. After doping with iodine was carried out, a linear relationship in the *I-V* characteristics was observed, suggesting that the partial oxidation of P3HT by iodine doping led to the macroscopically observed

conductivity of nanofibers [30]. The electronic conductivity of a single P3HT nanofiber was determined to be 122 ± 9 S/cm.

The P3HT nanofibers were collected onto an aluminum foil substrate on the rotating disc collector during the continuous electrospinning, and the aligned nanofiber assemblies (15 m thickness) could be peeled off of the aluminum foil (Figure 5.2b). The assemblies were not brittle and maintained their shape after removal from the substrates. The tensile strength of the aligned assembly along the nanofiber orientation direction was 4.6 ± 0.2 MPa and the degree of elongation at the break was 24.6 ± 2.2 %. The P3HT nanofibers within the free-standing assembly were loosely packed with a density of 0.27 g/cm^3. The nanofiber assemblies were cut into 2×2 cm^2 samples, and two electrodes were drawn at both edges of sample with silver paste to connect the nanofibers (Figure 5.2c). The resistance along the nanofiber orientation (type 1) was 7 times that in the direction orthogonal to the orientation (type 2), indicating the anisotropic conductivity in aligned nanofiber assemblies. Electron transport in the orthogonal direction requires contact with P3HT nanofibers in order to make pathways in nanofiber assemblies. Thus, the resistance depends on the number of contact positions among the P3HT nanofibers.

a)

b)

c)
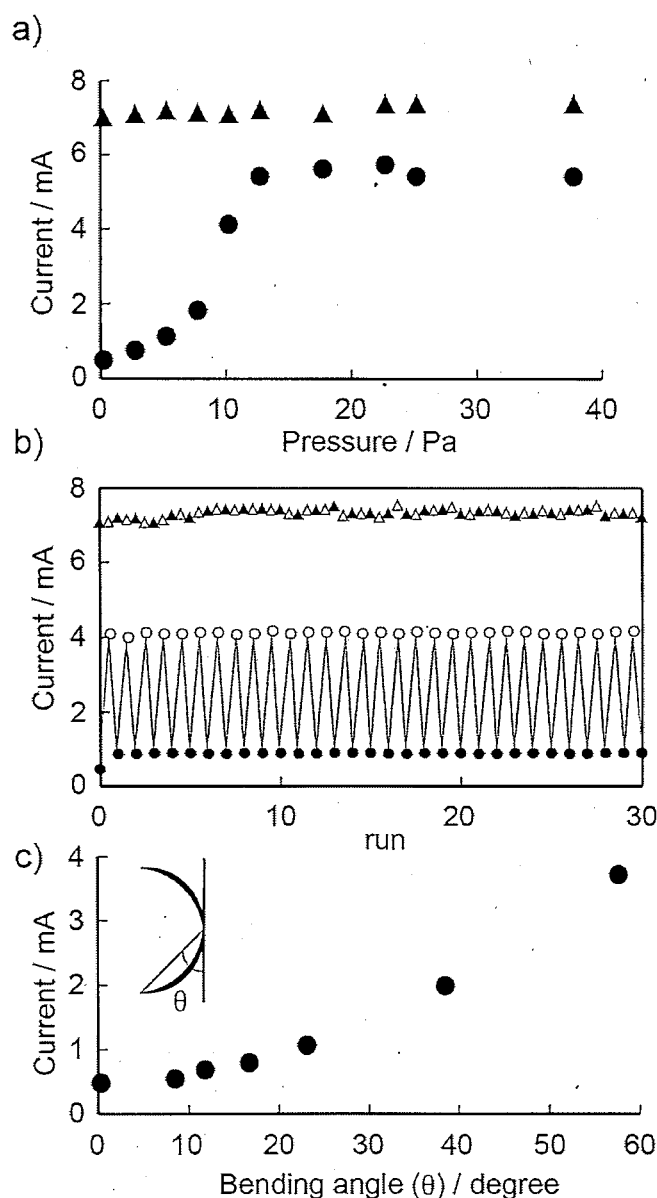
Figure 5.3 Electronic characterization of the sensor in response to pressure loads and bending. (a) Current changes from P3HT nanofiber assemblies possessing different arrangements of electrodes (▲: Type 1 and ● : Type 2) as a function of applied pressure. (b) Multiple-cycle test (30 cycles) of P3HT nanofiber assemblies (▲, △: Type 1 and ●, o : Type 2) with repeated loading (o and △) -unloading (● and ▲) of pressure at 10 Pa. (c) Current changes as a function of the bending angle.

The pressure-sensing properties of the P3HT nanofiber assemblies were investigated by measuring the current changes in response to different mechanical loads. The I-V measurements of assemblies showed ohmic behavior within a range of

0-5V, and the currents applied at 1.0 V between two electrodes on the assemblies were monitored. The currents between two electrodes parallel to the nanofiber axis within the assemblies were almost constant with increasing pressure. In contrast, the currents between the orthogonal electrodes increased steeply from 5 Pa and saturated above 15 Pa (Figure 5.3a). The minimum detectable pressure was as small as 3 Pa. We also performed multiple cycle tests by repeatedly loading and unloading pressure at 10 Pa (Figure 5.3b). The output signals in a direction orthogonal to the nanofiber orientation showed a constant value upon loading of pressure, and the current returned to the parent value at the unloading. While the current retuned to the parent value within 5 second after loading at 10 Pa, the returning needed over 30 min after loading at 30 Pa (Figure 5.4). When the nanofiber assemblies were compressed by the large loading, the nanofibers in the assemblies would be entangled and the releasing of entanglement requires a long period. The currents along the nanofiber orientation were almost constant, revealing no damage to nanofiber assemblies by applying pressure. When two ends of the nanofiber assembly were stuck to poly(ethylene terephthalate) (PET) film with the silver paste(Figure 5.5), the assembly could detect the bending angle by changing the currents (Figure 5.3c). Small physical inputs gave rise to additional contact among neighboring conductive nanofibers by the compression, which produced a decrease of the contact resistance in a direction orthogonal to the nanofiber orientation.
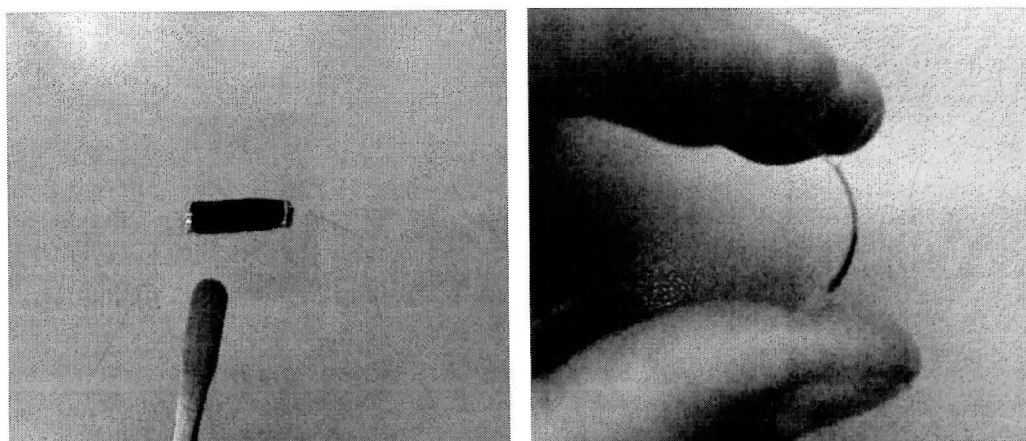
Figure 5.4 Photograph of P3HT nanofiber assembly for testing of sensing of bending motion. P3HT nanofiber assembly (length 2.0 cm, width 0.5 cm) attached with two electrodes in a direction orthogonal to the orientation was stick to PET film.The P3HT nanofiber assembly was deformed by bending of PET film.
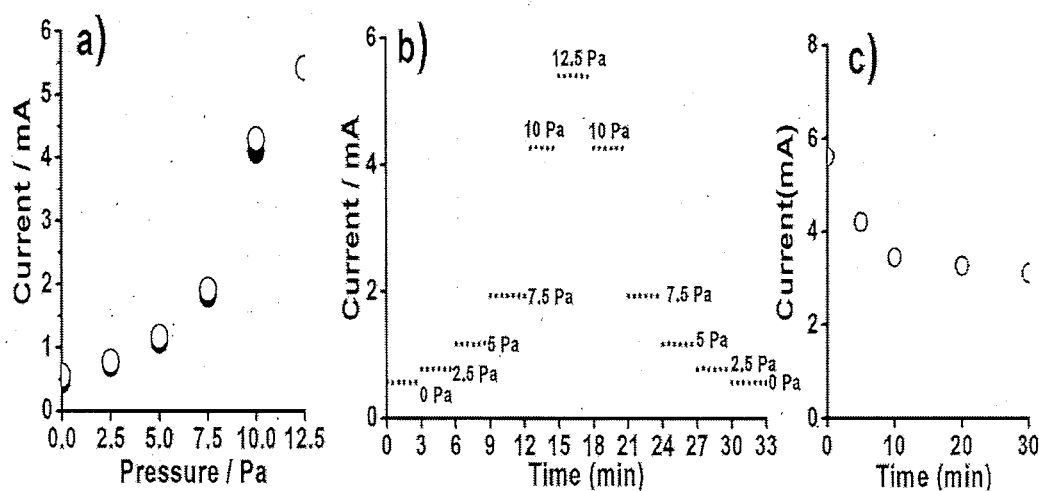
Figure 5.5 (a) Current changes from P3HT nanofiber assemblies as a function of applied pressure with loading (●) and unloading (○). (b) Current changes as a function of applied pressure with stepwise loading and unloading at 0, 2.5, 5, 7.5, 10.0, 12.5 Pa. (c) Current changes after loading at 30 Pa.

5.4 Conclusions

In summary, we have presented a flexible organic tactile sensor based on the reversible deformation of high-molecular-weight P3HT nanofibers within the aligned assemblies. The simple structure composed of aligned electrospun nanofibers can be used to develop tactile sensors for detecting small pressure changes and bending angles. We believe that the flexible devices based on simple nanofiber assemblies can be used as ambient sensors to monitor activities by embedding them within clothes and interiors. The sensing range of tactile sensors would depend on the diameter of the nanofibers within the assemblies. Although iodine doping can enhance the electronic conductivity of P3HT nanofibers, this conductivity cannot be maintained for a long period of time because of the evaporation of iodine from nanofibers. Work is currently underway in our laboratory to tune the sensing range by changing the nanofiber diameters and to enhance the durability of devices by using other dopants with greater environmental stability.

References

[1] Lakes R. *Nature*, **1993**, *361*, 511-515.

[2] Someya T, Sekitani T, Iba S, Kato Y, Kawaguchi H, Sakurai, T. *Proc. Natl. Acad. Sci.* U.S.A., **2004**, *101*, 9966-9970.

[3] Mannsfeld SCB, Tee BC, Stoltenberg RM, Chen CVH, Barman S, Muir BVO, Sokolov AN, Reese C, Bao Z. *Nat. Mater.*, **2010**, *9*, 859-864.

[4] Kim DH, Lu N, Ma R, Kim YS, Kim RH, Wang S, Wu J, Won SM, Tao H, Islam A, Yu KJ, Kim T, Chowdhury R, Ying M, Xu L, Li M, Chung HJ, Keum H, McCormick M, Liu P, Zhang YW, Omenetto FG, Huang Y, Coleman T, Rogers J A. *Science*, **2011**, 333, 838-843.

[5] Takei K, Takahashi T, Ho JC, Ko H, Gillies AG, Leu PW, Fearing RS, Javey A. *Nat. Mater.*, **2010**, *9*, 821-826.

[6] Lipomi DJ, Vosgueritchian M, Tee BC, Hellstrom SL, Lee JA, Fox CH, Bao Z. *Nat. Nanotech.*, **2011**, *6*, 788-792.

[7] Yamada T, Hayamizu Y, Yamamoto Y, Yomogida Y, Izadi-Najafabadi A, Futaba D N, Hata K. *Nat. Nanotech.*, **2011**, *6*, 296-301

[8] Pang C, Lee GY, Kim T, Kim SM, Kim HN, Ahn SH, Suh KY. *Nat. Mater.*, **2012**, *11*, 795-801.

[9] Wang C, Dong H, Hu W, Liu Y, Zhu D. *Chem. Rev.*, **2012**, *112*, 2208-2267.

[10] Cheng YJ, Yang SH, Hsu CS. *Chem. Rev.*, **2009**, *109*, 5868-5923.

[11] Merlo JA, Frisbie CD. *J. Polym. Sci. B: Polym. Phys.*, **2003**, *41*, 2674-2680.

[12] Kim FS, Ren G, Jenekhe SA. *Chem. Mater.*, **2011**, *23*, 682-732.

[13] González R, Pinto NJ. *Synth. Met.*, **2003**, *151*, 275-278.

[14] Greiner A, Wendorff JH. *Angew. Chem. Int. Ed.*, **2007**, *46*, 5670-5703.

[15] Laforgue A, Robitaille L. *Synth. Met.*, **2008**, *158*, 577-584.

[16] Pinto NJ, Carrasquillo KV, Rodd CM, Agarwal R. *Appl. Phys. Lett.*, **2009**, *94*, 083504.

[17] Chuangchote S, Fijita M, Sagawa T, Sakaguchi H, Yoshikawa S. *ACS Appl. Mater. Interfaces*, **2010**, *2*, 2995-2997.

[18] Lee SW, Lee HJ, Choi JH, Koh WG, Myoung JM, Hur JH, Park JJ, Cho JH, Jeong U. *Nano Lett.*, **2010**, *10*, 347-351.

[19] Yin K, Zhang L, Lai C, Zhong L, Smith S, Fong H, Zhu Z. *J. Mater. Chem.*, **2011**, *21*, 444-448.

[20] Kim T, Im JH, Choi HS, Yang SJ, Kim SW, Park CR. *J. Mater. Chem.*, **2011**, *21*, 14231-14239.

[21] Li D, Babel A, Jenekhe SA, Xia Y. *Adv. Mater.* **2004**, *16*, 2062-2066.

[22] Babel A, Li D, Xia Y, Jenekhe SA. *Macromolecules*, **2005**, *38*, 4705-4711. ·

[23] Lee S, Moon GD, Jeong U. *J. Mater. Chem.*, **2009**, 19, 743-748.

[24] Chen JY, Kuo CC, Lai CS, Chen WC, Chen HL. *Macromolecules*, **2011**, *44*, 2883-2892.

[25] Bedford NM, Dickerson MB, Drummy LF, Koerner H, Singh KM, Vasudev M C, Durstock MF, Naik RR. *Adv. Energy Mater.*, **2012**, *2*, 1136-1144.

[26] Chan KHK, Yamao T, Kotaki M, Hotta S. *Synth. Met.*, **2010**, *160*, 2587-2595.

[27] Samitsu S, Shimomura T, Heike S, Hashizume T, Ito K. *Macromolecules*, **2008**, *41*, 8000-8010.

[28] Pal S, Nandi AK. *J. Appl. Polm. Sci.*, **2006**, *101*, 3811-3820.

[29] Dudenko D, Kiersnowski A, Shu J, Pisula W, Sebastiani D, Spiess HW, Hansen MR. *Angew. Chem. Int. Ed.*, **2012**, *51*, (DOI: 10.1002/anie.201205075).

[30] McCullough R, Tristram-Nagle S, Williams SP, Lowe RD, Jayaraman M. *J. Am. Chem. Soc.*, **1993**, *115*, 4910-4911.

CHAPTER 6 Summary and prospective for future research

6.1 Findings

Fibers, like paper and plastic, are some of the cheapest and most widely used flexible substrates. One of their interesting features is that they can be weaved or integrated into yarns of different colors to form a large variety of complex, two-dimensional (2D), or three-dimensional (3D) patterns. Aside from their main use in clothing, ropes, curtains, and other daily objects, fibers and textiles have recently been considered as potential substrates for low-cost flexible electronics and multifunctional fabrics, commonly referred to as electronic fibers (e-fibers) or electronic textiles (e-textiles or smart textiles). Therefore, fibers have other functions in addition to those based on their intrinsic material properties.

Chapter 2 the electrospinning process of polyvinyl alcohol (PVA) aqueous solutions for two samples (HS and FL) was carried out. FL solutions produced nanofibers in electrospinning process, whereas HS solutions showed poorer electrospinning process accompanying dropping and electrospraying. The analysis of the spinning solution properties indicated that the electric conductivity and viscosity of both FL and HS solutions demonstrated similar behaviors. However, the surface tensions of FL solutions were slightly decreased while the surface tension presented U-shaped curves for HS solutions with the increase of polymer concentration. The NMR spetra and DSC results implied that HS had higher degree of saponification. The metal element analysis results meant that HS contained high concentrations of calcium and aluminum ions while FL much less. The dosage of calcium chloride into FL aqueous solutions indicated that electrospinning process was significantly aggravated. The electrospinning process of HS was substantially improved both by dialysis and complexation. It was the high degree of saponification and it was intramolecular cross-linking and intermolecular cross-linking occurred between PVA chain and the metal ions that coined the abnormal behaviors in surface tension and thus deteriorated electrospinning process.

Chapter 3 the production of superfine polyvinyl alcohol (PVA) fiber is usually much difficult by using the routine spinning, whereas electrospinning is a viable

technique since the mechanism of fiber formation was different. In this paper, the effects of solution properties in terms of the residual acetyl group and high valence metal ion impurity of PVA on electrospinning were carefully investigated. Both the solution viscosity and the surface tension tendencies with PVA concentration indicated that there existed strong physico-chemical interaction besides concentration and molar mass factors. NMR spectra and DSC thermographs indirectly showed that the devoid acetyl group of PVA would promote the physical gelation and the formation of hydrogen bonding, and the physical crosslinking occurred at high saponification degrees in the presence of high valence metal ion impurity. All the interactions aggravated the electrospinning process. Nevertheless, both removal of high valence metal ion impurity and the selection of PVA with low saponification degrees would be always accessible routes to ensure the PVA electrospinning.

Chapter 4 fully hydrolyzed PVA nanofibers were successfully prepared by the electrospinning method using PVA aqueous solutions in the presence of acetic acid. Acetic acid is a vaporous additive to reduce the surface tension and enhance the electronic conductivity of PVA aqueous solution. The adjustment of solution properties of PVA aqueous solutions resulted in the continuous spinning of uniform nanofibers. The concentration of acetic acid and the molecular weight of PVA strongly affected the resulted morphology of PVA nanofibers. The post-thermal treatment of PVA nanofibers and the *in-situ* cross-linking greatly enhanced the water resistance of nanofibers. Especially, the morphology of cross-linked PVA nanofibers did not change after immersing into hot water. Furthermore, the tensile mechanical properties of PVA nanofiber nonwovens were significantly enhanced via cross-linking. The decoration of magnetite nanoparticles onto the surface of the cross-linked nanofibers was demonstrated. The nanofibers with magnetite showed the same morphology as the parent nanofibers and revealed a magnetic property. The cross-linked PVA nanofibers can open new possibility for the creation of functional nanocomposite materials by combining various nanomaterials.

Chapter 5 described a flexible organic tactile sensor based on reversible deformation of high-molecular-weight P3HT nanofibers within the aligned assemblies. The simple structure composed of aligned electrospun nanofibers can be used to develop tactile sensors for detecting small pressure changes and bending angles. We believe that the flexible devices based on simple nanofiber assemblies can be used as ambient sensors to monitor activities by embedding them within

clothes and interiors.

In summary, new specialties of electrospun nanofibers; high absorption capability of metal ions and sensing small pressure were disclosed. Tough cross-linked PVA nanofibers which can maintain nanofibrous morphology in hot water and play as a good template for nanoparticles deposition was successfully achieved. Meanwhile, flexible tactile sensor based on aligned P3HT nanofibers was successfully fabricated. All these results suggested that the smart nanofibrous nonwovens fabricated by electrospinning have potential applications for future textiles and devices.

6.2 Prospective for future research

In this thesis, the experimental results showed new specialties of electrospun nanofibers; high absorption capability of metal ions to form nanoparticles in hydrothermal synthesis and small pressure-sensing properties. These specialties might be original from the small diameter of nanofiber and could be adjusted by altering the diameter. Based on these, smart nanofibrous nonwovens via electrospinning will open new applications of textiles in the future.

For my study, there are still some follow-up experiments should be done in the future.

1. Experimental results indicated the crosslinked PVA nanofibers can play as a good template for deposited nanoparticles. Further characterations are essential for clear the mechanism and the distribution of deposited nanoparticles.

2. Aligned P3HT fibers showed good sensing properties for tactile sensor. Addtional efforts should be carried out for improving the crystallinity and doping method of P3HT nanofibers.

3. Efforts should be carried out to explore new techniques for electrospinnning spinnerets to increase the productivity of the conventional setup.

List of Publications

1. **Qiang Gao**, Junko Takizawa, and Mutsumi Kimura. Hydrophilic non-wovens made of cross-linked fully-hydrolyzed poly(vinyl alcohol) electrospun nanofibers. *Polymer*, **2013**, *54*, 120-126.

2. **Qiang Gao**, Hikaru Meguro, Shuji Okamoto, Mutsumi Kimura. Flexible tactile sensor using the reversible deformation of poly(3-hexylthiophene) nanofiber assemblies. *Langmuir*, **2012**, *28*, 17593-17596

3. Jian Zhou, **Qiang Gao**, Tadashi Fukawa, Hirofusa Shirai and Mutsumi Kimura, Macroporous conductive polymer films fabricated by electrospun nanofiber templates and their electromechanical properties. *Nanotechnology*, **2011**, *22*, 275501(8pp).

4. Xinsheng Zhu, **Qiang Gao**, Detai Xu, Xiaoli Shi. Effect of interaction between hydroxyl group and high valence metal ion impurity on the electrospinnability of polyvinyl alcohols, *Journal of Applied Polymer Science*, **2009**, *113*, 143-149.

5. Xinsheng Zhu, **Qiang Gao**, Yong Xu, Detai Xu. Improvement of the electrospinnability of Polyvinyl alcohol via dialysis and complexation pretreatment. *Journal of Polymer Research*, **2007**, *14*, 277-282.

Conferences

1. **Qiang Gao**, Mutsumi Kimura, Hirofusa Shirai. Smart membrane made of cross-linked PVA nanofibers. Fiber preprints, Japan, Vol. 65 (2010), No.1 (Annual Meeting) (Tokyo, Japan) (Oral)

2. **Qiang Gao**, Mutsumi Kimura, Hirofusa Shirai. *In-situ* cross-linking of electrospun PVA nanofibers. International Conference of Future Textile 2010, July 15-17, 2010, P121 (Shinshu university, Ueda, Japan) (Poster)

3. **Qiang Gao**, Tadashi Fukawa, Mutsumi Kimura, Hirofusa Shirai. Aligned Electrospun

Nanofibers for Nanogenrators. The 2011 International Symposium on Molecular Systerms~Global COE Symposium for Young Researchers. May 9-11, 2011. P12, (The Luigans, Fukuoka, Japan) (Poster)

4. **Qiang Gao**, Tadashi Fukawa, Mutsumi Kimura, Hirofusa Shirai. Pb-free Ceramic Nanofibrous Assemble via Electrospinning. 11th Asian Textile Conference, November 1-4, 2011, P103, (Daegu, Korea) (Oral)

5. **Qiang Gao**, Tadashi Fukawa, Mutsumi Kimura, Hirofusa Shirai. Nanofibrous Assembles via Electrospinning for Nanogenerators. The 6th International Conference on Advanced Fiber /Textile Materials 2011. Dec7-9, 2011. P17 (Shinshu university, Ueda, Japan) (Poster, **Excellent Poster Award**)

Acknowledgements